Progress in Limiting Strategy:

From One-dimensional Concepts to Multi-dimensional Limiting Process


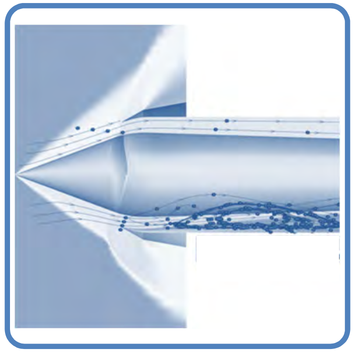
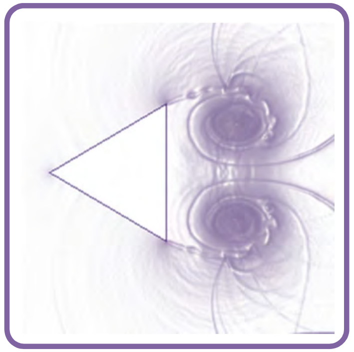

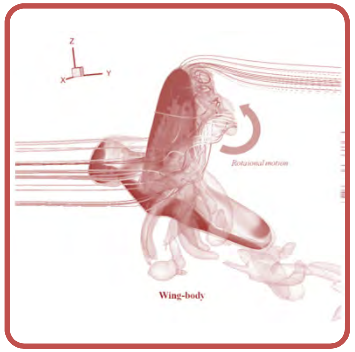

Chongam Kim

Department of Aerospace Engineering

Seoul National University, Korea

11, November, 2013

Computational Fluid Dynamics

- **A Discipline to Solve Conservation Laws of Fluid Dynamics Numerically.**
  - **Flow information**
    - → pressure, velocity, temperature…
    - → force (lift, drag) & moment or heat flux distribution
  - **Multidisciplinary design optimization and Flow control**
    - → performance improvement
  - **Input data**
    - Structural design
    - Engine performance
    - S&C, and so on

- **Numerical Discretization**
  - **FDM, FEM, and FVM**
- **Finite Volume Discretization**
  - **Directly apply the integral form of the conservation laws to each computational cell in physical domain.**
  - **One-step conservative finite volume discretization for 1-D Euler eqns.**

$$\mathbf{U}_t + \mathbf{F(U)}_x = \mathbf{0} \text{ with } \mathbf{U} = \begin{bmatrix} \rho \\ \rho u \\ \rho E \end{bmatrix},\ \mathbf{F}(\mathbf{U}) = \begin{bmatrix} \rho u \\ \rho u^2 + p \\ \rho u H \end{bmatrix},\ \begin{bmatrix} E = e + \dfrac{u^2}{2} \\ H = h + \dfrac{u^2}{2} \end{bmatrix},\ p = (\gamma - 1)\rho\left[E - \frac{u^2}{2}\right],\ \gamma = 1.4$$

From $\int_{t^n}^{t^{n+1}} \int_{x_{j-1/2}}^{x_{j+1/2}} (\mathbf{U}_t + \mathbf{F(U)}_x) dx dt = \mathbf{0}$, we have

$$\int_{x_{j-1/2}}^{x_{j+1/2}} \mathbf{U}(x, t^{n+1})\, dx - \int_{x_{j-1/2}}^{x_{j+1/2}} \mathbf{U}(x, t^n)\, dx = -\left(\int_{t^n}^{t^{n+1}} \mathbf{F}\left[\mathbf{U}(x_{j+1/2}, t)\right] dt - \int_{t^n}^{t^{n+1}} \mathbf{F}\left[\mathbf{U}(x_{j-1/2}, t)\right] dt \right)$$

Seeking a solution in an average sense over $\Delta x = [x_{j-1/2}, x_{j+1/2}]$, $\Delta t = [t^n, t^{n+1}]$

by introducing $\mathbf{U}_j^n = \dfrac{1}{\Delta x} \displaystyle\int_{x_{j-1/2}}^{x_{j+1/2}} \mathbf{U}(x, t^n)\, dx$, $\hat{\mathbf{F}}_{j+1/2}^n = \dfrac{1}{\Delta t} \displaystyle\int_{t^n}^{t^{n+1}} \mathbf{F}\left[\mathbf{U}(x_{j+1/2}, t)\right] dx$,

We have $\mathbf{U}_j^{n+1} = \mathbf{U}_j^n - \dfrac{\Delta t}{\Delta x}\left(\hat{\mathbf{F}}_{j+1/2}^n - \hat{\mathbf{F}}_{j-1/2}^n\right)$ with $\hat{\mathbf{F}}_{j+1/2}^n = \hat{\mathbf{F}}_{j+1/2}^n(\mathbf{U}_j^n, \mathbf{U}_{j+1}^n)$.

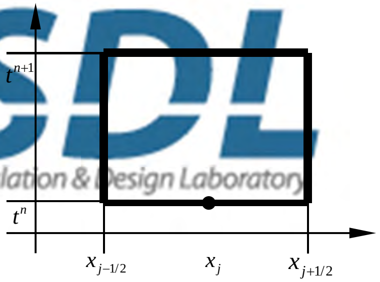

Monotone Scheme

- **Some conditions for an entropy-satisfying weak solution**
  - **Consistency**
    - $\hat{f}(u,u) = f(u)$
    - Lipschitz continuity

      $$\left|\hat{f}(u_{j-1},u_j) - f(u)\right| \le L\max\left(\left|u_{j-1}-u\right|,\left|u_j-u\right|\right)$$
  - **Conservation**
    - $\hat{f}_{j+1/2,L} = \hat{f}_{j+1/2,R}$
  - **Monotonicity**
    - Monotone scheme (Harten-Hyman-Lax, 1987)

      $$u_j^{n+1} = u_j^n - \frac{\Delta t}{\Delta x}(\hat{f}_{j+1/2} - \hat{f}_{j-1/2}) = H_j(u_{j+k},\ldots,u_j,\ldots,u_{j-k}),$$

      $$\frac{\partial H_j}{\partial u_{j+l}} \ge 0, \quad \forall |l| \le k.$$
      - Consider 3-point scheme

        $$u_j^{n+1} = u_j^n - \frac{\Delta t}{\Delta x}(\hat{f}_{j+1/2} - \hat{f}_{j-1/2}) = H_j(u_{j-1},u_j,u_{j+1}) \text{ with } \hat{f}_{j+1/2} = \hat{f}_{j+1/2}(u_j,u_{j+1})$$

        $\dfrac{\partial H_j}{\partial u_{j+l}} \ge 0$ gives $\hat{f}_{j+1/2}(u,v)$ is monotonically increasing/decreasing with respect to u / v.

- **Computed results**
  - Conservative and non-conservative scheme

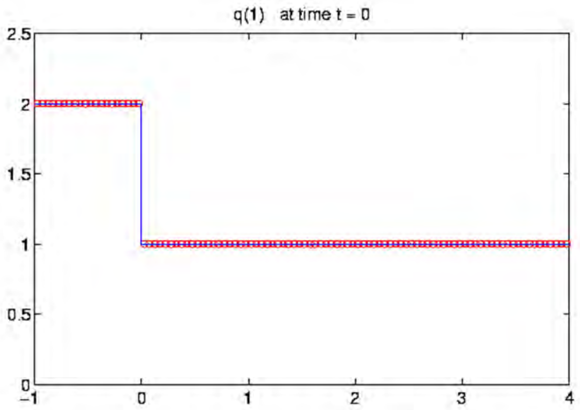

< Conservative scheme >

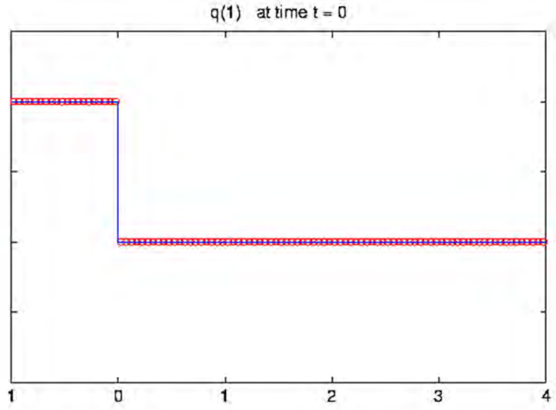

< Non-conservative scheme >

  - Monotone and non-monotone scheme

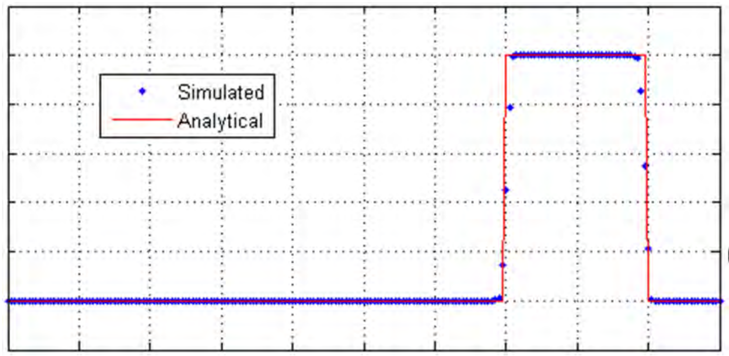

< Monotone scheme >

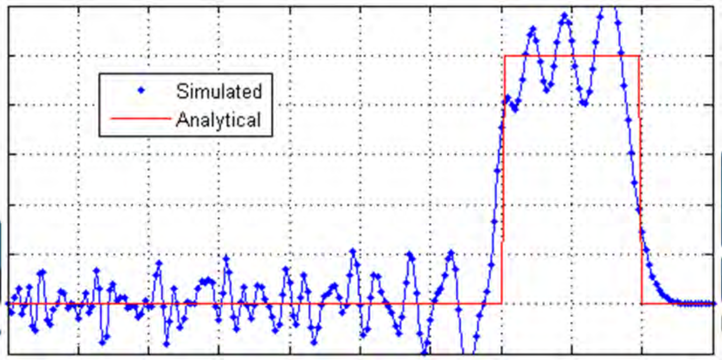

< Non-monotone scheme >

Non-linear Stability and Hyperbolic PDE

- Gibb's Phenomenon and Monotonicity
- Non-linear Stability
- Oscillation Control Strategies

- **Gibb's Phenomenon (1899)**
  - **Approximation of a profile including discontinuity by Fourier Series (or interpolating techniques based on global basis functions)**
    - Numerical oscillations across discontinuity with *O(1)* → It never dies out even if the number of basis function is increasing.

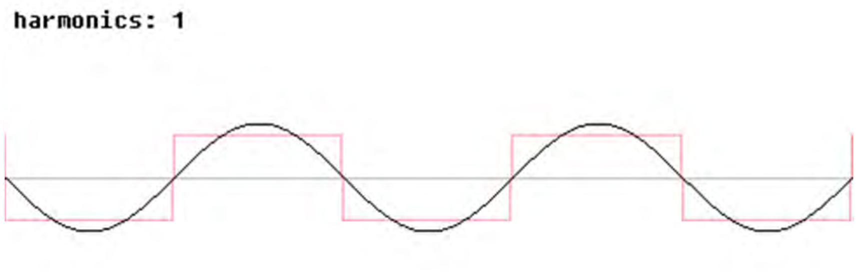

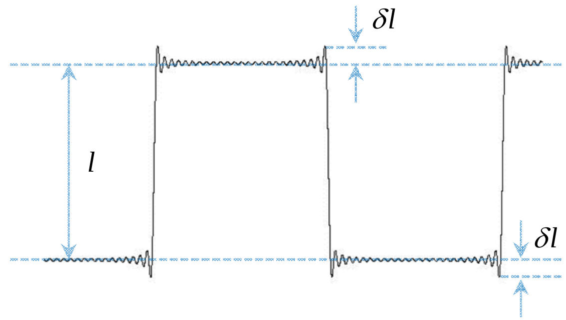

< Animation of the Gibbs phenomenon >

- **Magnitude of overshoot/undershoot** $(\delta l\,/\,l) \sim \pm 14\%$
- **Locally converge (or L_1, L_2 convergence) but not uniformly (L_∞ convergence)** **→ warning to naive capturing of discontinuities by increasing the number of interpolating function or mesh point**

- **First-order Scheme and Numerical Diffusion**
  - **For $u_t + au_x = 0$ with Upwind or L-F scheme**
  - **Modified equation**

$$u_t + au_x = \begin{cases} \dfrac{\Delta x^2}{2\Delta t}\left(1-\sigma^2\right)u_{xx} & \text{for L-F} \\ \dfrac{a\Delta x}{2}\left(1-\sigma^2\right)u_{xx} & \text{for upwind} \end{cases}$$

$$\Rightarrow u_t + au_x = c_1(\Delta x, \Delta t)u_{xx} \text{ with } \sigma = a\frac{\Delta t}{\Delta x}$$

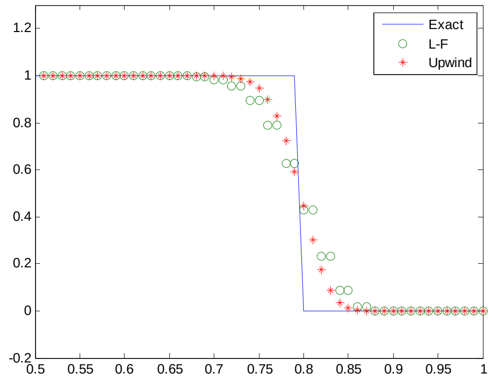

  - **Leading error term is numerically dissipative → a smooth transition without oscillations**
    - Excessive numerical dissipation
      - Unacceptable loss of accuracy → Too many grid points
      - Viscous computation and resolution of boundary layer

Gibb's Phenomenon and Monotonicity (Cont')

- **Second-order Scheme and Numerical Dispersion**
  - **Modified equation of L-W and B-W scheme**

$$u_t + a u_x = \begin{cases} -\dfrac{a\Delta x^2}{6}\left(1-\sigma^2\right)u_{xxx} & \text{for L-W} \\ \dfrac{a\Delta x^2}{6}\left(2-3\sigma+\sigma^2\right)u_{xxx} & \text{for B-W} \end{cases}$$

$$\Rightarrow u_t + a u_x = c_1 u_{xxx} \xrightarrow[u=\hat{u}(w)e^{iwx}]{FT} \hat{u}(\omega,t)_t + i\left(a\omega + c_1\omega^3\right)\hat{u}(\omega,t) = 0$$

$$\Rightarrow \hat{u}(\omega,t) \sim e^{-i\left(a\omega+c_1\omega^3\right)t} \quad \text{vs.} \quad \hat{u}_{ex}(\omega,t) \sim e^{-ia\omega t}$$

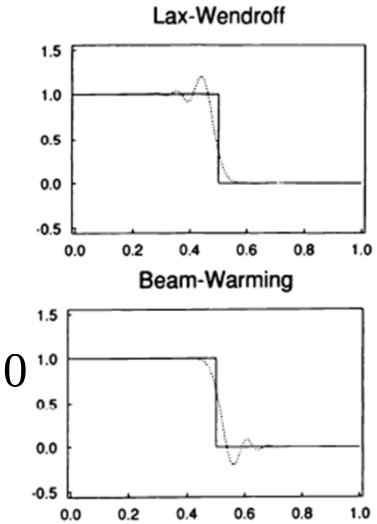

  - **Numerical dispersion relation:** $a(\omega) = a\omega + c_1\omega^3$
    For each Fourier component with ω, group velocity $a_g(\omega) \equiv da(\omega)/d\omega$

    $a_g(\omega) = a + 3c_1\omega^2 \approx a$ for small wave number (long wave length)

    $\neq a$ for large wave number (short wave length)

    if $a > 0, c_1 < 0$ for $L-W \Rightarrow$ lagging error

    $c_1 > 0$ for $B-W \Rightarrow$ leading error

  - **Numerical oscillations across discontinuity regardless of central differencing or upwinding once the order of accuracy is greater than one.**

Non-linear Stability

- **Godunov Barrier Theorem on Monotonicity**
  - **(Godunov, 1959)** ***For the fully discretized 'linear' scheme of*** $u_j^{n+1} = Lu_j^n \equiv \sum_q c_{jq} u_{j+q}^n$ ***, it can not be better than first-order accurate if the scheme is maximum-norm bounded.***
    - (Positivity condition) If L is stable in maximum-norm, c_{jq} should be non-negative (or $\dfrac{du_j^{n+1}}{du_{j+q}^n} \geq 0$).
      - The monotonicity condition by HHL can be recovered.
- **Observation**
  - **To obtain more than 2nd-order monotone scheme, the scheme should be non-linear even for linear equation.**
    - $c_{jq}(\Delta x, \Delta t) \;\Rightarrow\; c_{jq}(\Delta x, \Delta t, u_{j+q}^n)$
  - **Limiting strategy to realize higher-order accuracy and oscillation-free profile is essential.**
- **Non-linear Stability Criteria**
  - **Stability using L_1 norm**
    - Total Variation Diminishing (TVD) and Total Variation Bounded (TVB)
  - **Stability using L_∞ norm**
    - Discrete maximum principle
      - Local Extremum Diminishing (LED)

Non-linear Stability (Cont')

- **Total Variation Stability**
  - **A way to connect non-linear stability with the convergence of a computed solution**

    $$TV(u) \equiv \int_{-\infty}^{\infty} |u'(x)|\, dx \quad \text{or} \quad TV(u) \equiv \sum_{j=-\infty}^{\infty} |u_j - u_{j-1}| = 2\left(\sum \text{maxima} - \sum \text{minima}\right)$$

    - A useful tool to measure local oscillation
  - **A monotone scheme is TVD, and a TVD scheme is monotonicity-preserving.**
    - 3-point TVD formulation of $TV(u^{n+1}) \leq TV(u^n)$ (Harten, 1983)
  - **TVB allows oscillation only if it does not grow unboundedly.**
    - $TV(u^{n+1}) \leq (1+\alpha\Delta t) TV(u^n)$
    - TVB may avoid clipping at extrema but badly influences convergence.
- **Discrete Maximum Principle**
  - **Edge-based local space-time discrete maximum principle**
    - (Barth, 2003) For a fully-discrete scheme of $u_j^{n+1} = u_j^n + \frac{\Delta t}{|T_j|} \sum_{\forall e_{jk} \in \partial T_j} C_{jk}(u_h^n)(u_k^n - u_j^n)$

$$\min_{\forall e_{jk} \in \partial T_j} (u_k^n, u_j^n) \leq u_j^n \leq \max_{\forall e_{jk} \in \partial T_j} (u_k^n, u_j^n) \Rightarrow \min_{\forall e_{jk} \in \partial T_j} (u_k^n, u_j^n) \leq u_j^{n+1} \leq \max_{\forall e_{jk} \in \partial T_j} (u_k^n, u_j^n)$$

If $C_{jk}(u_h^n) \geq 0$ for $\forall e_{jk} \in \partial T_j$, and $1 - \frac{\Delta t}{|T_j|} \sum_{\forall e_{jk} \in \partial T_j} C_{jk}(u_h^n) \geq 0$ (CFL-like condition)

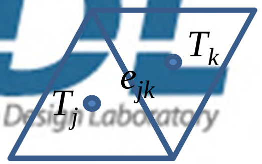

Oscillation Control Strategies

- **Remarkable Oscillation Control Strategies since 1970s**
  - **Flux Corrected Transport (FCT)**
    - Boris (1973), Zalesak (1984)
  - **MUSCL and Geometric Subcell Reconstruction**
    - Van Leer (1977, 1979)
  - **Total Variation Diminishing (TVD) / Total Variation Bounded (TVB)**
    - Harten (1983), Sweby (1984), Shu (1987)
  - **Essentially Non-Oscillatory (ENO) / Weighted ENO (WENO)**
    - Harten and Shu et al. (1987), Liu et al. (1994)
  - **Spekreijse's Monotonic Concept**
    - Spekreijse (1989)
  - **Multi-dimensional Reconstruction with Slope Limiter**
    - Barth (1989, 1990)
  - **Local Extremum Diminishing (LED)**
    - A. Jameson (1993)
  - **Adaptive Stencil Reconstruction (ENO/WENO)**
    - Abgrall (1993), Shu (1999)

One-dimensional Limiting Strategies

- Flux Corrected Transport
- TVD Scheme using Flux Limiter
- MUSCL and Slope Limiter
- ENO/WENO Schemes

- **Flux Corrected Transport (FCT) Method and Flux Limiter**
  - **The first algorithm that recognized the consequence of Godunov's theorem and presented a non-linear way of limiting the cell-interface flux**
  - **For** $u_t + au_x = 0$ with $u_j^{n+1} = u_j^n - \frac{\Delta t}{\Delta x}\left(F_{j+1/2} - F_{j-1/2}\right)$

$$\text{Design } F_{j+1/2} \quad s.t. \quad F_{j+1/2} = \begin{cases} \text{2nd-order in smooth region} \\ \text{1st-order across local extrema} \end{cases}$$

$$\Rightarrow \text{Let } \begin{cases} F_{j+1/2}^H : \text{a 2nd-order 'non-monotonic' flux} \\ F_{j+1/2}^L : \text{a 1st-order 'monotonic' flux} \end{cases}$$

$$F_{j+1/2} = F_{j+1/2}^L + \alpha_{j+1/2}\left(F_{j+1/2}^H - F_{j+1/2}^L\right) \text{ with } \alpha_{j+1/2} \begin{cases} \approx 1 \text{ for smooth region} \\ \approx 0 \text{ near local extrema} \end{cases}$$

  - **Procedure**
    - S1) Compute $F_{j+1/2}^L,\ F_{j+1/2}^H$ from u_j^n
    - S2) Define 'anti-diffusive' flux as $\tilde{F}_{j+1/2} = F_{j+1/2}^H - F_{j+1/2}^L = d_{j+1/2}^L - d_{j+1/2}^H = \varepsilon \Delta u_{j+1/2}^n \ (\varepsilon = \varepsilon^L - \varepsilon^H > 0)$
    - S3) Obtain the intermediate lower-order (or 1st-order) 'monotonic' solution

$$\bar{u}_j = u_j^n - \frac{\Delta t}{\Delta x}\left(F_{j+1/2}^L - F_{j-1/2}^L\right)$$

    - S4) Correct $\tilde{F}_{j+1/2}$ s.t. the final updated solution (u_j^{n+1}) is free of extrema not found in $\bar{u}_j^n$ or u_j^n

$$F_{j+1/2}^c \equiv \alpha_{j+1/2}\tilde{F}_{j+1/2} = \alpha_{j+1/2}\left(d_{j+1/2}^L - d_{j+1/2}^H\right) \text{ with } 0 \le \alpha_{j+1/2} \le 1$$

Flux Corrected Transport

- S5) Update the final solution with the corrected flux $F^c_{j+1/2}$

$$u_j^{n+1} = \bar{u}_j - \frac{\Delta t}{\Delta x}\left(F^c_{j+1/2} - F^c_{j-1/2}\right) = u_j^n - \frac{\Delta t}{\Delta x}\left\{ \left[F^L_{j+1/2} + \alpha_{j+1/2}\left(F^H_{j+1/2} - F^L_{j+1/2}\right)\right]_{j+1/2} - [\ldots]_{j-1/2} \right\}$$

- S6) The corrected flux $F^c_{j+1/2}$ is designed as

$$F^c_{j+1/2} = \min\bmod\left(\frac{\Delta x}{\Delta t}\Delta\bar{u}_{j-1/2}, \tilde{F}_{j+1/2}, \frac{\Delta x}{\Delta t}\Delta\bar{u}_{j+3/2}\right)$$

- The anti-diffusive flux is controlled such that it does not create new local extrema.
  - Updated soln. satisfies the monotonic constraint in terms of the intermediate distribution

$$\min(\bar{u}_{j-1}, \bar{u}_j, \bar{u}_{j+1}) \le u_j^{n+1} \le \max(\bar{u}_{j-1}, \bar{u}_j, \bar{u}_{j+1})$$

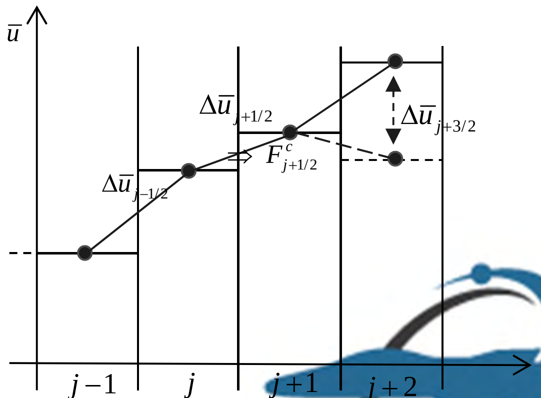

< Determination of the corrected flux >

Flux Corrected Transport (Cont')

- **Example**
  - Linear advection problem with smooth and discontinuous profiles

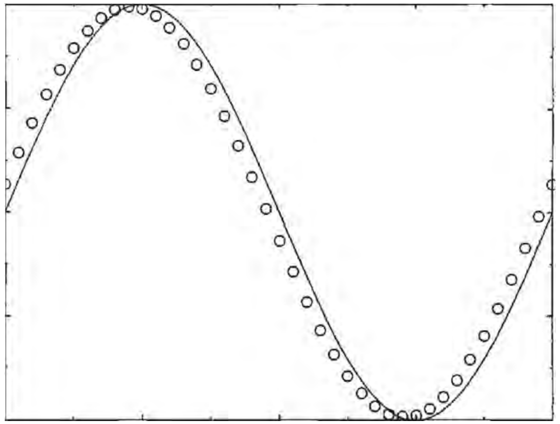

Lax-Wendroff method for test case 1

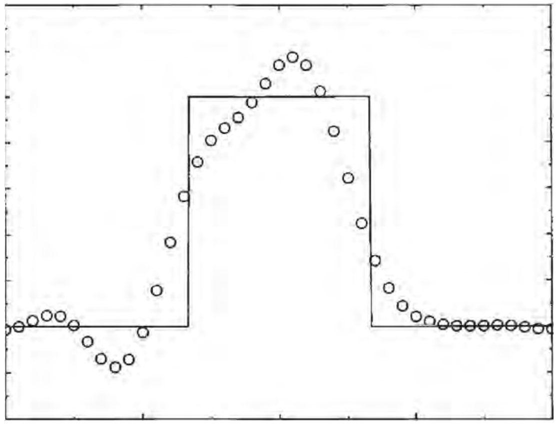

Lax-Wendroff method for test case 2

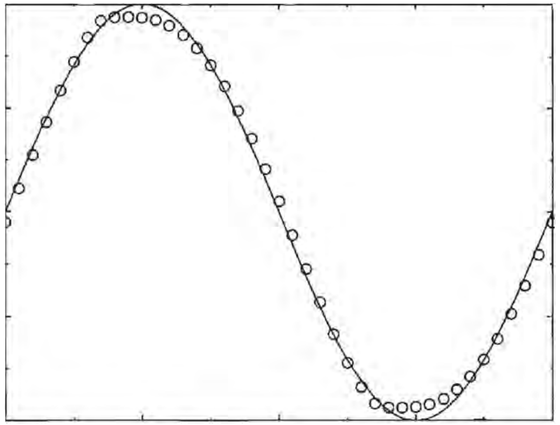

FCT method for test case 1

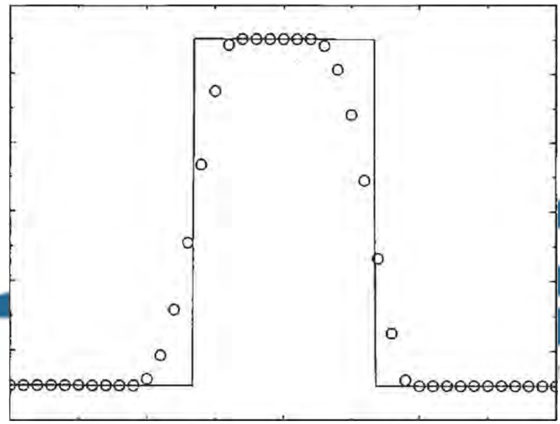

FCT method for test case 2

TVD Scheme using Flux Limiter

- **TVD Schemes and One-step Flux Limiting Function**
  - **A Class of one-step scheme using refined form of flux limiters and satisfying TVD property**
    - The limited flux form is assumed as $F_{j+1/2} = F^L_{j+1/2} + \phi_j \left(F^H_{j+1/2} - F^L_{j+1/2} \right).$

      ϕ_j is a limiter function monotoring the behavior of local solution u_j^n.
    - For $u_t + au_x = 0$ with $a > 0$, consider $F^H_{j+1/2}$ as the L-W flux, and $F^L_{j+1/2}$ as the upwind flux

$$
\begin{aligned}
u_j^{n+1} &= u_j^n - \frac{\sigma}{2}\left(u_{j+1}^n - u_{j-1}^n\right) + \frac{\sigma^2}{2}\left(u_{j+1}^n - 2u_j^n + u_{j-1}^n\right) \\
&= u_j^n - \sigma\left(u_j^n - u_{j-1}^n\right) - \frac{\sigma(1-\sigma)}{2}\left(u_{j+1}^n - 2u_j^n + u_{j-1}^n\right) \\
&= u_j^n - \frac{\Delta t}{\Delta x}\left(F_{j+1/2} - F_{j-1/2}\right)
\end{aligned}
$$

$$
\Rightarrow F_{j+1/2} = \underbrace{au_j^n}_{\text{upwind}} + \underbrace{\frac{a(1-\sigma)}{2}\Delta u_{j+1/2}^n}_{\text{Lax-Wendroff correction}}
$$

Thus, the limited flux form is $F_{j+1/2} = au_j + \dfrac{a(1-\sigma)}{2}\Delta u_{j+1/2}\phi_j$ with $\phi_j \geq 0$.

    - Define $r_j = \Delta u_{j-1/2} / \Delta u_{j+1/2}$ to measure the change of local slope (or total variation) and design $\phi_j = \phi(r_j)$ with the TVD principle

TVD Scheme using Flux Limiter

Three-pint TVD condition

- The three-point scheme of the form $u_j^{n+1} = u_j^n - C_{j-1/2}\Delta u_{j-1/2}^n + D_{j+1/2}\Delta u_{j+1/2}^n$ is TVD
  if $C_{j-1/2},\ D_{j+1/2} \geq 0,$ and $C_{j+1/2} + D_{j+1/2} \leq 1$ for $\forall j.$
- The flux limited from of L-W scheme satisfies the TVD condition is satisfied if

$$\text{we have } \phi(r) \text{ s.t. } \begin{cases} 0 \leq \dfrac{\phi(r)}{r} \leq 2 \text{ and } 0 \leq \phi(r) \leq 2, \text{ if } r \geq 0 \\ \phi(r) = 0, \text{ if } r < 0 \text{ (to prevent the accentuation of local extrema)} \end{cases}$$

TVD region and limiters

- $\phi(\mathrm{r})_{r=1}=1$ to get a smooth transition with second-order accuracy
- Convex combination of L-W and B-W is desirable to avoid
  too much compression (region *B*) or too much diffusion (region *C*).
- Some TVD limiters
  - superbee limiter: $\phi(r) \ = \ \max\{0,\ \min(1,2r),\ \min(r,2)\}$
  - van Leer limiter: $\phi(r) \ = \ (|r|+r)/(1+|r|)$
  - MC limiter: $\phi(r) \ = \ \max\{0,\ \min((1+r)/2, 2, 2r)\}$
  - minmod limiter: $\phi(r) \ = \ \min(1, r)$

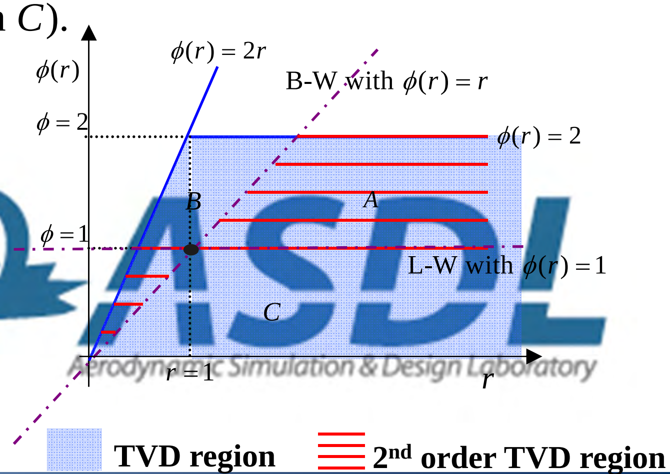

TVD Scheme using Flux Limiter (Cont')

- **Example**
  - Linear advection problem with smooth and discontinuous profiles

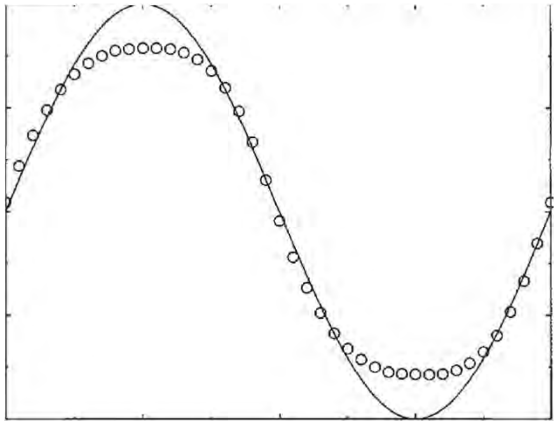

Flux-limited method with minmod limiter

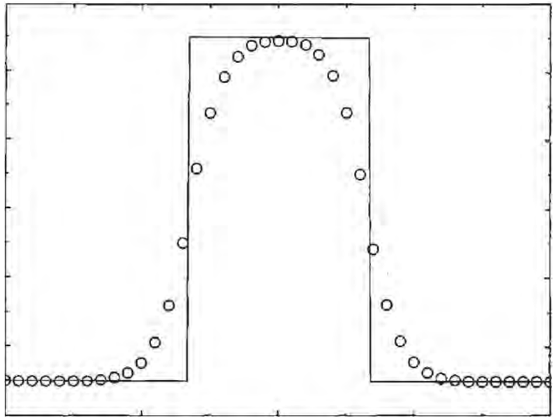

Flux-limited method with minmod limiter

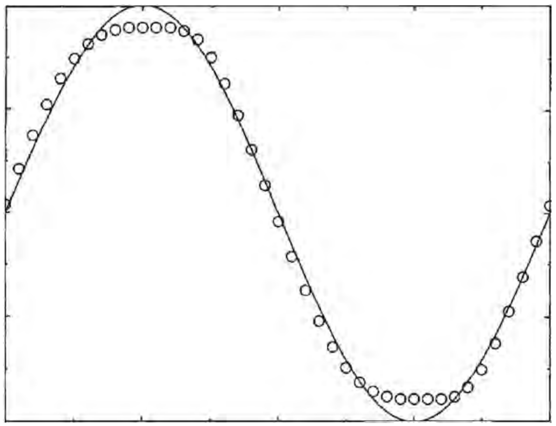

Flux-limited method with van Leer limiter

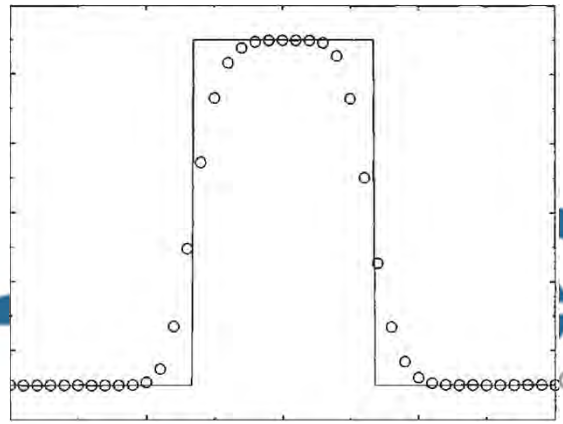

Flux-limited method with van Leer limiter

TVD Scheme using Flux Limiter (Cont')

- **Example**
  - Linear advection problem with smooth and discontinuous profiles

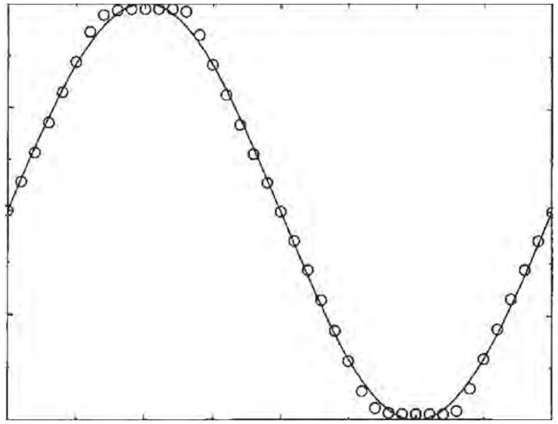

Flux-limited method with superbee limiter

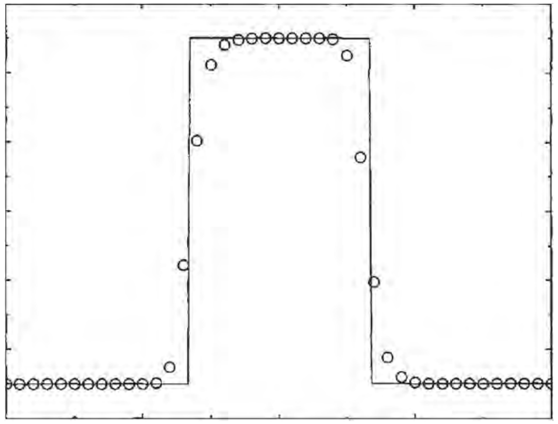

Flux-limited method with superbee limiter

  - Accuracy preservation in both smooth and discontinuous region

MUSCL and Slope Limiter

- **Geometric Approach for Monotonic Schemes**
  - **Numerical scheme is analyzed in terms of reconstruction, evolution and projection stage.**
    - Ex) Flow physics of first-order upwind scheme for $u_t + au_x = 0$, $a > 0$

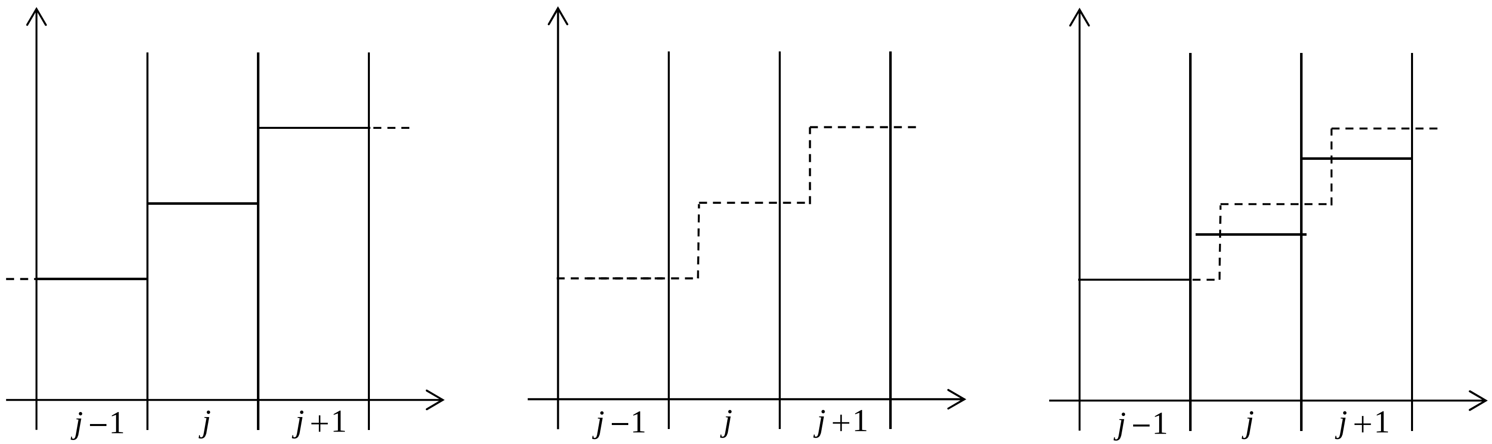

< Reconstruction > **< Evolution >** **< Projection >**

- Reconstruction stage: approximation of exact initial distribution from cell-averaged values
- Evolution stage: reconstructed initial profile is convected $\Delta s_x = a \cdot \Delta t$ by $u_t + au_x = 0$.
- Projection stage: projection of the convected profile to update a new cell-averaged solution at $t^{n+1} = t^n + \Delta t$

MUSCL and Slope Limiter (Cont')

- Evolution and projection stages are not handled numerically.
- A higher-order monotonic scheme via a higher-order reconstruction of the initial data with the monotonic constraint
- Sub-cell distribution for second-order schemes

$$u(x) = u_j + \left(\frac{\partial u}{\partial x}\right)_j (x - x_j) + \left(\frac{\partial^2 u}{\partial x^2}\right)_j \frac{(x - x_j)^2}{2} + O(\Delta x^3)$$

$$\cong u_j + \frac{\Delta u_j}{\Delta x}(x - x_j), \quad x_{j\text{-}1/2} \le x_j \le x_{j+1/2} \quad \text{with} \quad u_j = \int_{x_{j-1/2}}^{x_{j+1/2}} u(x)\,dx$$

  - Estimation of the local slope Δu_j

- **Second-order upwind scheme with monotonicity**

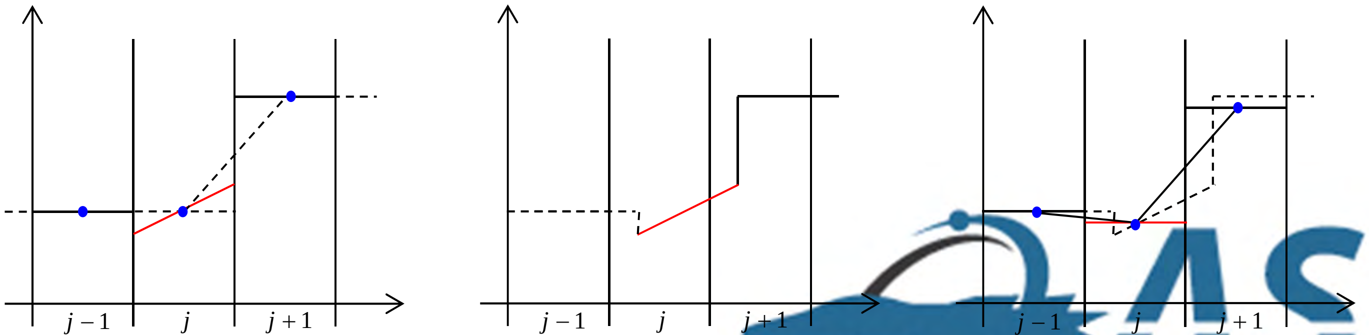

- Non-monotonic estimation of the local slope (Δu_j) creates a new (artificial) local maxima/minima.

MUSCL and Slope Limiter (Cont')

- If $TV(u(x)) \le TV(u^n)$ in reconstruction stage, the whole stages are TVD, since evolution and projection stages are intrinsically total variation not increasing.
- Slope limiters to satisfy the monotonic subcell distribution
  - $\Delta u_j\big|_{\min} = \min\left(\Delta u_{j+1/2}, \Delta u_{j-1/2}\right)$ • $\Delta u_j\big|_{sb} = \max\left(\Delta u_{i1}, \Delta u_{i2}\right)$

    with $\Delta u_{i1} = \min\left(\Delta u_{j+1/2}, 2\Delta u_{j-1/2}\right), \Delta u_{i2} = \min\left(\Delta u_{j-1/2}, 2\Delta u_{j+1/2}\right)$
  - $\Delta u_j\big|_{MC} = \min\left(\dfrac{\Delta u_{j+1/2} + \Delta u_{j-1/2}}{2}, 2\Delta u_{j+1/2}, 2\Delta u_{j-1/2}\right)$

MUSCL schemes with slope limiters

- First-order upwinding: $\hat{f}_{j+1/2} = \frac{1}{2}\left(f_j + f_{j+1}\right) - \frac{\left|a_{j+1/2}\right|}{2}\Delta u_{j+1/2}$
- Sub-cell linear distribution using slope limiters: $u(x) = u_j + \frac{\Delta u_j}{\Delta x}\left(x - x_j\right), \quad x_{j-1/2} \le x \le x_{j+1/2}$

  $\rightarrow u_{jR} = u\left(x_{j+1/2}\right) = u_j + \frac{\Delta u_j}{2}$ and $u_{jL} = u\left(x_{j-1/2}\right) = u_j - \frac{\Delta u_j}{2}$ to replace u_j and u_{j+1}
- Interface flux using the interpolated values: $\hat{f}_{j+1/2} = \frac{1}{2}\left(f_L + f_R\right) - \frac{\left|a_{j+1/2,\,L/R}\right|}{2}\Delta u_{j+1/2,\,L/R}$

ENO/WENO Schemes

- **Essentially Non-Oscillatory Higher-order Interpolation Procedure**
  - **TVD vs. ENO**
    - (TVD scheme) Locally first-order accurate across all extrema to strictly enforce monotonicity → accuracy loss across smooth extrema with excessive diffusion or clipping
    - (TVD scheme) A fixed stencil (3-point TVD scheme with $u_j, u_{j\pm1}$)
      → difficult to obtain a higher-order TVD scheme
    - (ENO scheme) Allow the increase of local extrema up to the order of truncation error to achieve higher-order accuracy across smooth extrema
    - (ENO scheme) Locally adaptive smooth stencil for higher-order interpolation
  - **Procedure to construct ENO stencil (or locally adaptive stencil)**
    - Cell-averaged value or flux function
  - **ENO polynomial reconstruction using cell-averaged value, u_i**
    - Step 1. Introduce Newton's divided difference based on cell-averaged values

$$u[x_i] \equiv u_i,\ u[x_i, x_{i+1}] \equiv \{u[x_{i+1}] - u[x_i]\}/\Delta x = (u_{i+1} - u_i)/\Delta x, \ldots,$$

$$u[x_i, x_{i+1}, \ldots, x_{i+k}] \equiv \{u[x_{i+1}, x_{i+2}, \ldots, x_{i+k}] - u[x_i, x_{i+1}, \ldots, x_{i+k-1}]\}/(k\Delta x)$$

If flow field is sufficiently smooth, $u[x_i, x_{i+1}, \ldots, x_{i+k}] = \dfrac{1}{k!}\dfrac{d^k u}{dx^k}\Big|_{\xi},\ x_i \le \xi \le x_{i+k}$

ENO/WENO Schemes (Cont')

- Step 1. Introduce Newton's divided difference based on cell-averaged values

  And, if $u(x)$ has a jump discontiuity of the l-th derivative at $x = x_p$,

$$u[x_i, x_{i+1}, \ldots, x_{i+k}] = O\left(\frac{1}{\Delta x^{k-l}}\left(\frac{d^l u(x_p^+)}{dx^l} - \frac{d^l u(x_p^-)}{dx^l}\right)\right), \quad x_i \le \xi \le x_{i+k}$$

- Step 2. Compare each divided difference to determine ENO stencil successively

$$\text{Starting from the cell } i, \text{ take} \begin{cases} i+1 & \text{if } \left|u[x_i, x_{i+1}]\right| \le \left|u[x_{i-1}, x_i]\right| \\ i-1 & \text{if } \left|u[x_i, x_{i+1}]\right| > \left|u[x_{i-1}, x_i]\right| \end{cases}$$

$$\Rightarrow u(x) = u_i + u[x_j, x_{j+1}](x - x_i), \quad x_{j-1/2} \le x \le x_{j+1/2} \quad \text{(linear reconstruction)}$$

$$\text{with } j = \begin{cases} i & \text{if } \left|u[x_i, x_{i+1}]\right| \le \left|u[x_{i-1}, x_i]\right| \\ i-1 & \text{if } \left|u[x_i, x_{i+1}]\right| > \left|u[x_{i-1}, x_i]\right| \end{cases}$$

- Step 3. ENO stencil in a recursive manner

  For $m = 0, 1, 2, \ldots, n-1$ with $l_0(i) = i$,

$$l_{m+1}(i) = \begin{cases} l_m(i) & \text{if } \left|u[x_{l_m(i)}, x_{l_m(i)+1}, \ldots, x_{l_m(i)+m+1}]\right| \le \left|u[x_{l_m(i)-1}, x_{l_m(i)}, \ldots, x_{l_m(i)+m}]\right| \\ l_m(i)-1 & \text{if } \left|u[x_{l_m(i)}, x_{l_m(i)+1}, \ldots, x_{l_m(i)+m+1}]\right| > \left|u[x_{l_m(i)-1}, x_{l_m(i)}, \ldots, x_{l_m(i)+m}]\right| \end{cases}$$

ENO/WENO Schemes (Cont')

- Step 3. ENO stencil in a recursive manner

  From $\left[x_{l_m(i)}, x_{l_m(i)+1}, \ldots, x_{l_m(i)+m}\right]$ with $0 \le m \le n$, construct a n-th order ENO polynomial as

$$u_n(x) = u[x_{l_n(i)}] + u[x_{l_n(i)}, x_{l_n(i)+1}]\left(x - x_{l_n(i)}\right) + u\left[x_{l_n(i)}, x_{l_n(i)+1}, x_{l_n(i)+2}\right]\left(x - x_{l_n(i)}\right)\left(x - x_{l_n(i)+1}\right) + \ldots$$

$$+ u[x_{l_n(i)}, x_{l_n(i)+1} \ldots, x_{l_n(i)+n}]\left(x - x_{l_n(i)}\right)\left(x - x_{l_n(i)+1}\right)\ldots\left(x - x_{l_n(i)+n-1}\right)$$

$$\Rightarrow u(x) = \sum_{j=0}^{n} u\left[x_{l_n(i)}, x_{l_n(i)+1}, \ldots, x_{l_n(i)+j}\right] \prod_{k=0}^{j-1}\left(x - x_{l_n(i)+k}\right), \quad x_{j-1/2} \le x \le x_{j+1/2}$$

  - With the conservation constraint of $\int_{x_{i-1/2}}^{x_{i+1/2}} u(x) = u_i$, it can be shown that

    $TV\left(u^{n+1}\right) \le TV\left(u^n\right) + O\left(\Delta x^r\right)$ for $r-th$ order ENO interpolation,

    if there are at least $(r+1)$ smooth points between local smooth extrema.

- **ENO interpolation using flux function, f_i**
  - Step 1. Start from first-order flux (mostly, Lax-Friedrich flux)

$$f_i = f_i^+ + f_i^- \text{ with } f_i^+ \equiv \frac{1}{2}\left(f_i + \alpha u_i\right),\ f_i^- \equiv \frac{1}{2}\left(f_i - \alpha u_i\right), \alpha \ge \max_{u \in [u_i, u_{i+1}]} \left|\partial f / \partial u\right|$$

    the cell-interface flux is obtained by $\hat{f}_{i+1/2} = f_i^+ + f_{i+1}^- = [(f_i + f_{i+1}) - \alpha \Delta u_{i+1/2}]/2.$

  - Step 2. Carry out the same piecewise polynomial reconstruction using $f_i^{\pm}$

$$u\left[x_i, x_{i+1}, \ldots, x_{i+k}\right] \rightarrow f^{\pm}\left[x_i, x_{i+1}, \ldots, x_{i+k}\right] \Rightarrow \hat{f}_{i+1/2} = \left(f_{iL}^+ + f_{(i+1)R}^-\right)/2$$

ENO/WENO Schemes (Cont')

- **Characteristics of ENO scheme**
  - Pure interpolation not limiting technique → accuracy preservation across smooth extrema
  - Adaptive smoothest stencil of ENO scheme could be changed by a small perturbation at round-off level → convergence and accuracy problem

- **Weighted ENO (WENO) Scheme**
  - **Smoothness indicator is introduced for non-linear weighting coefficients.**
  - **WENO polynomial reconstruction using cell-averaged value, u_i**
    - Step 1. Interpolation on global/local stencil

      Reconstruct $k-th$ degree polynomial $p_j(x)$ on S_j and $2k-th$ degree polynomial $Q(x)$ on $T=\sum_j S_j$ as

      $$\bar{u}_{i+l}=\int_{I_{i+l}} p_j(x)dx/\Delta x_{i+l},\ (l=-k+j,...,j) \text{ and } \bar{u}_{i+l}=\int_{I_{i+l}} Q(x)dx/\Delta x_{i+l},\ (l=-k,...,k)$$

      Find linear weights such that $Q(x_{i+1/2})=\sum_{j=0}^{k}\gamma_j p_j(x_{i+1/2})$

    - Step 2. For each cell S_j, local smoothness is measured by the indicator.

      $$\beta_j=\sum_{l=1}^{k}\int_{x_{i-1/2}}^{x_{i+1/2}}\Delta x^{2l-1}\left(\frac{\partial^l}{\partial^l x}p_j(x)\right)^2 dx$$

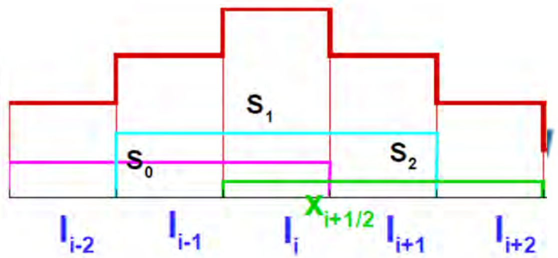

ENO/WENO Scheme (Cont')

- Step 3. Non-linear weights to satisfy the ENO property
  - If the stencil S_j is in smooth region: $\omega_j = O(1)$
  - If the stencil S_j is in non-smooth region: $\omega_j \le O(h^k)$

  Compute the nonlinear weights based on the smoothness indicator

$$\bar{\omega}_j = \frac{\gamma_j}{(\varepsilon + \beta_j)^2} \quad \text{and} \quad \omega_j = \frac{\bar{\omega}_j}{\sum_l \bar{\omega}_l}$$

- Step 4. *(2k+1)-th* degree WENO reconstruction via convex combination with the non-linear weights

$$R_i(x) = \sum_{j=0}^{k} \omega_j p_j(x) \;\Rightarrow\; u_{iR} = R_i\left(x_{i+1/2}\right),\;\; u_{iL} = R_i\left(x_{i-1/2}\right)$$

ENO/WENO Schemes (Cont')

- **Example**

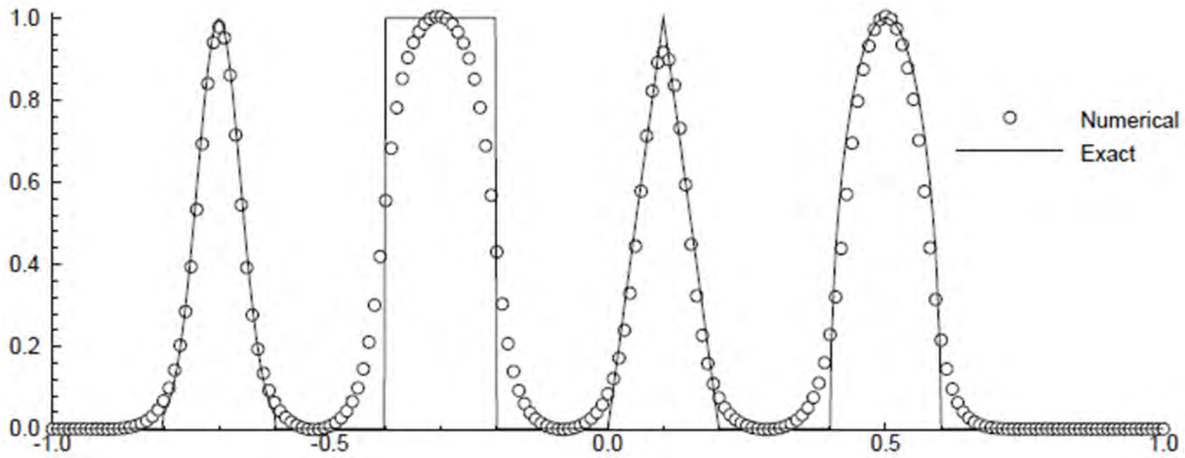

< ENO 4th-order >

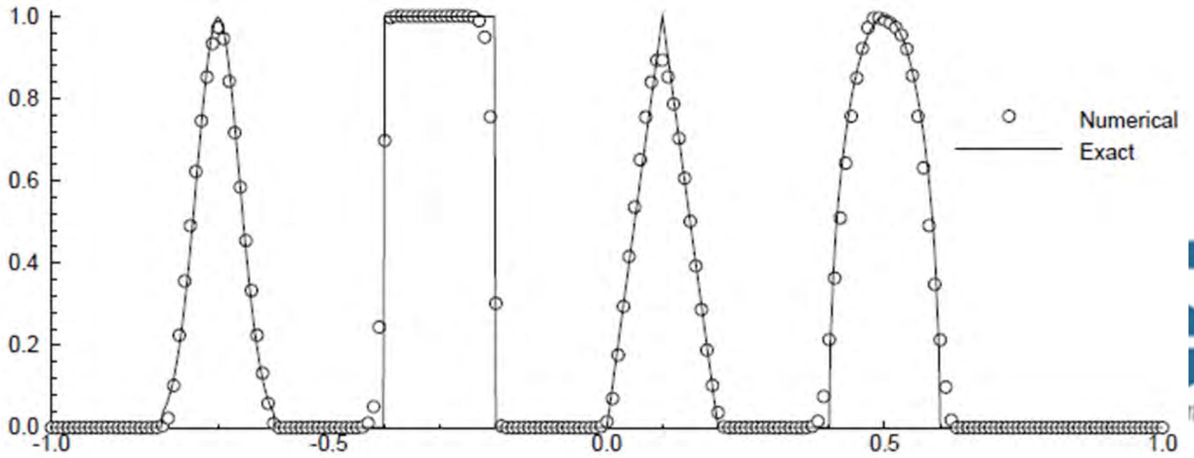

< WENO 5th-order >

Multi-dimensional Limiting Process

- Problems in Multi-dimensional Extension
- Limiting Condition on Multiple Dimensions
- Formulation of MLP on Structured Grids
- Maximum Principle and MLP Condition
- Numerical Results

Problems in Multi-dimensional Extension

- **Critical Survey**
  - **Analyses based on one-dimensional flow physics**
    - 1-D SCL of $\frac{\partial u}{\partial t}+\frac{\partial f(u)}{\partial x}=0$ with $f(u)=au, \frac{u^2}{2} \Rightarrow \frac{d\bar{u}_j}{dt}=-\frac{1}{\Delta x}(\hat{f}_{j+1/2}-\hat{f}_{j-1/2})$
    - Monotonicity constraint on $u_{j+1/2}$: $\min(\bar{u}_j,\bar{u}_{j+1}) \le u_{j+1/2} \le \max(\bar{u}_j,\bar{u}_{j+1})$
  - **Multi-dimensional extension**
    - 2-D SCL of $\frac{\partial u}{\partial t}+\frac{\partial f(u)}{\partial x}+\frac{\partial g(u)}{\partial y}=0 \Rightarrow \frac{d\bar{u}_{i,j}}{dt}=-\frac{1}{\Delta x}(\hat{f}_{i+1/2,j}-\hat{f}_{i-1/2,j})-\frac{1}{\Delta y}(\hat{g}_{i,j+1/2}-\hat{g}_{i,j-1/2})$
    - Monotonicity constraint by dimensional splitting:

$$\left.\begin{array}{l}(x\text{-}dir)\ \min(\bar{u}_{i,j},\bar{u}_{i+1,j}) \le u_{i+1/2,j} \le \max(\bar{u}_{i,j},\bar{u}_{i+1,j})\\ (y\text{-}dir)\ \min(\bar{u}_{i,j},\bar{u}_{i,j+1}) \le u_{i,j+1/2} \le \max(\bar{u}_{i,j},\bar{u}_{i,j+1})\end{array}\right\} \Rightarrow \left\{\begin{array}{l}\text{Is it good enough to handle multi-}\\ \text{dimensional flow situation?}\end{array}\right.$$

  - **Two-peaks and one-ridge problem (Jameson, 1995)**
    - For $TV(\bar{u})=\int_V \|\nabla \bar{u}\|_p\, ds$ with $p=1,\ 2,\ \infty$

      $TV_{two-peaks} < TV_{one-ridge}$
    - 2-D TVD scheme is at most first-order accurate (Goodman and LeVeque, 1985)

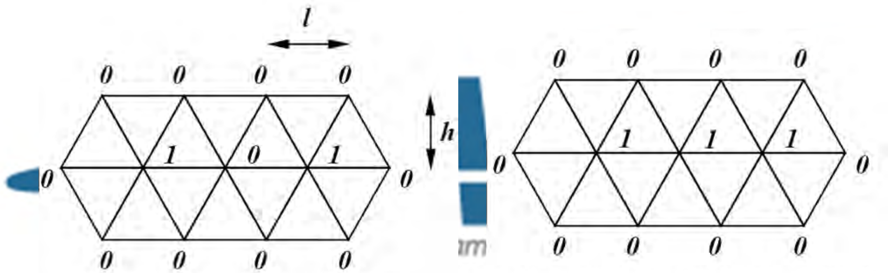

Two Peaks: $TV = 4+2\sqrt{3}\ (L_1),\ 6\ (L_2)$, or $2+2\sqrt{3}\ (L_\infty)$.

One Ridge: $TV = 6+\sqrt{3}\ (L_1),\ 7\ (L_2)$, or $5+3\sqrt{3}\ (L_\infty)$.

Problems in Multi-dimensional Extension (Cont')

- **Dimensional splitting extension is not sufficient to control numerical oscillations in multiple dimensions.**
  - **Dimensional splitting TVD schemes do not guarantee monotonicity at vertex (Kim & Kim, 2005 / Yoon & Kim, 2008)**
- **Limiting strategy in Non Grid-aligned Distributions**
  - **Dimensional splitting approach cannot handle local extrema at vertex**

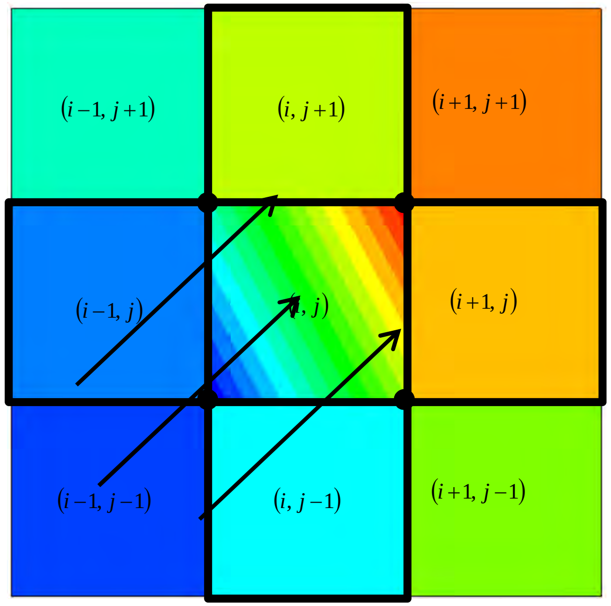

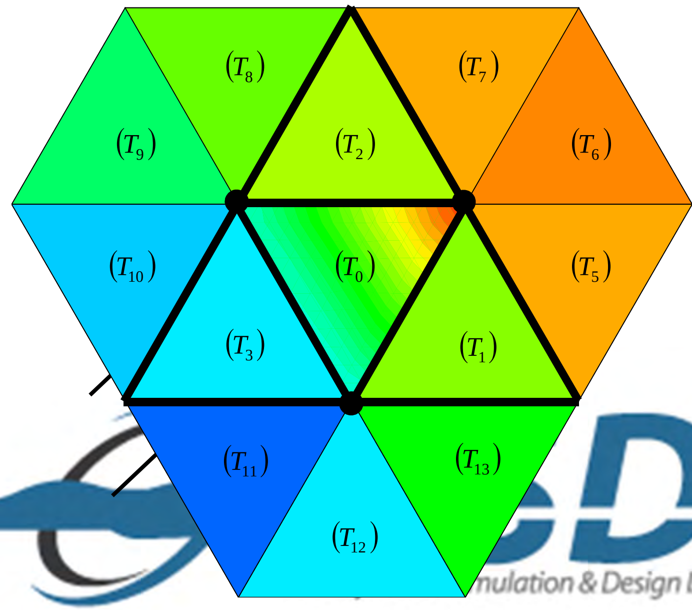

< [illegible] >

Limiting Condition on Multiple Dimensions

- **Multiple Dimensional Limiting Condition:** $\bar{u}_{neighbor}^{\min} \le u \le \bar{u}_{neighbor}^{\max}$
  - **MLP Condition on 2-D and 3-D Structured Grids**

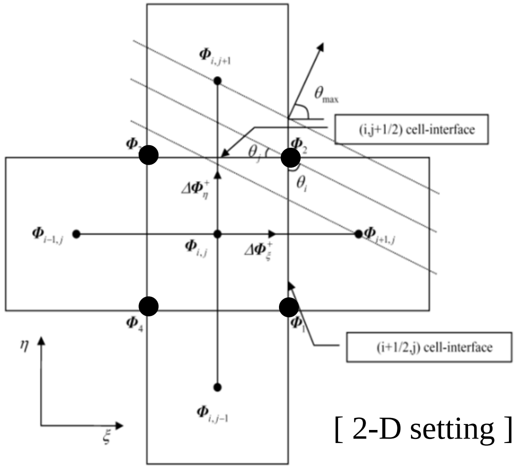

[2-D setting]

$$\min\left(\bar{u}_{i,j},\bar{u}_{i+1,j},\bar{u}_{i,j-1},\bar{u}_{i+1,j-1}\right) \le u_1 \le \max\left(\bar{u}_{i,j},\bar{u}_{i+1,j},\bar{u}_{i,j-1},\bar{u}_{i+1,j-1}\right)$$

$$\cdots$$

$$\min\left(\bar{u}_{i,j},\bar{u}_{i-1,j},\bar{u}_{i,j+1},\bar{u}_{i-1,j+1}\right) \le u_4 \le \max\left(\bar{u}_{i,j},\bar{u}_{i-1,j},\bar{u}_{i,j+1},\bar{u}_{i-1,j+1}\right)$$

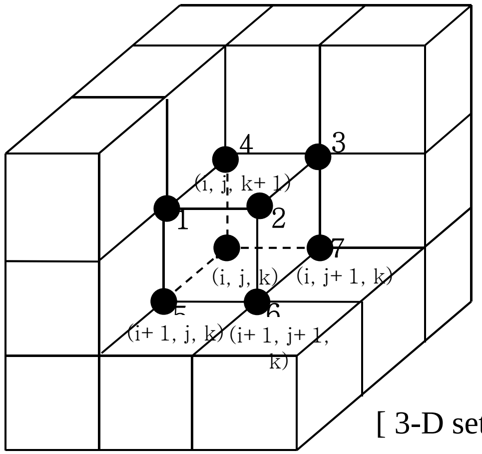

[3-D setting]

$$\min\begin{pmatrix}\bar{u}_{i,j,k}, & \bar{u}_{i+1,j,k}, & \bar{u}_{i,j-1,k}, & \bar{u}_{i+1,j-1,k}, \\ \bar{u}_{i,j,k+1}, & \bar{u}_{i+1,j,k+1}, & \bar{u}_{i,j-1,k+1}, & \bar{u}_{i+1,j-1,k+1}\end{pmatrix} \le u_1 \le \max\begin{pmatrix}\bar{u}_{i,j,k}, & \bar{u}_{i+1,j,k}, & \bar{u}_{i,j-1,k}, & \bar{u}_{i+1,j-1,k}, \\ \bar{u}_{i,j,k+1}, & \bar{u}_{i+1,j,k+1}, & \bar{u}_{i,j-1,k+1}, & \bar{u}_{i+1,j-1,k+1}\end{pmatrix}$$

$$\cdots$$

$$\min\begin{pmatrix}\bar{u}_{i,j,k}, & \bar{u}_{i-1,j,k}, & \bar{u}_{i,j+1,k}, & \bar{u}_{i-1,j+1,k}, \\ \bar{u}_{i,j,k+1}, & \bar{u}_{i-1,j,k-1}, & \bar{u}_{i,j+1,k-1}, & \bar{u}_{i-1,j+1,k-1}\end{pmatrix} \le u_8 \le \max\begin{pmatrix}\bar{u}_{i,j,k}, & \bar{u}_{i-1,j,k}, & \bar{u}_{i,j+1,k}, & \bar{u}_{i-1,j+1,k}, \\ \bar{u}_{i,j,k+1}, & \bar{u}_{i-1,j,k-1}, & \bar{u}_{i,j+1,k-1}, & \bar{u}_{i-1,j+1,k-1}\end{pmatrix}$$

Formulation of MLP on Structured Grids

- **TVD-MUSCL vs. MLP on Structured Mesh**

$$u^L_{i+1/2,j} = \overline{u}_{i,j} + 0.5\phi(r_L)\Delta\overline{u}_{i-1/2,j}$$

$$u^R_{i+1/2,j} = \overline{u}_{i+1,j,k} - 0.5\phi(r_R)\Delta\overline{u}_{i+3/2,j}$$

$$\text{with } r_L = \frac{\Delta\overline{u}_{i+1/2,j}}{\Delta\overline{u}_{i-1/2,j}}, r_R = \frac{\Delta\overline{u}_{i+1/2,j}}{\Delta\overline{u}_{i+3/2,j}}$$

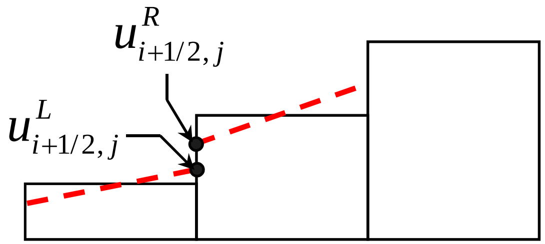

- **Limiting region**
  - $\phi(r) = \max(0, \min(2, 2r))$: TVD limiting region based on 1-D analysis
  - $\phi(r) = \max(0, \min(\alpha, \alpha r))$: MLP limiting region for multi-dimensional flows

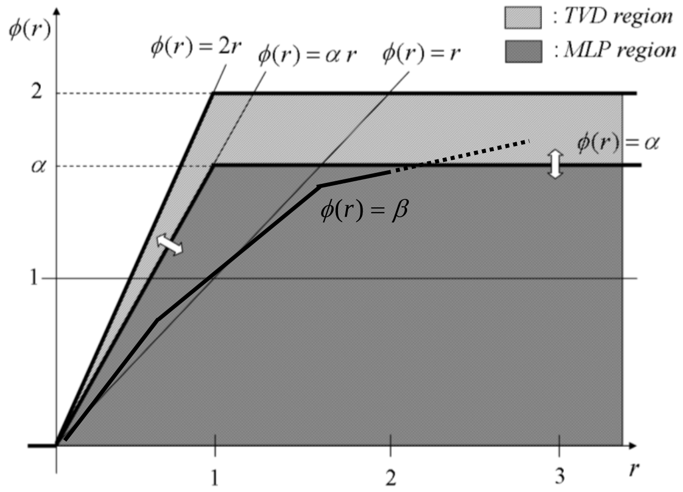

[TVD vs. MLP region]

- **MLP limiting function**
  - $\phi(r) = \max(0, \min(\alpha, \alpha r, \beta))$ with

    α: multi-dimensional restriction coefficient determining the upper bound of MLP region

    β: local slope obtained from subcell interpolation function

Formulation of MLP on Structured Grids (Cont')

- **Determination of Multi-dimensional Restriction Coefficient, *α***
  - **Step 1. Assume a cell-vertex value estimated by**

$$u_{i+1/2,j+1/2} = \bar{u}_{i,j} + \Delta u^{x}_{i+1/2,j} + \Delta u^{y}_{i,j+1/2} = \bar{u}_{i,j} + \left(1 + r_{xy}\right)\Delta u^{x}_{i+1/2,j} \text{ with } r_{xy} = \Delta u^{y}_{i,j+1/2} \big/ \Delta u^{x}_{i+1/2,j}$$

  - • Note that we only need to check the upper bound of the maximum vertex value and the lower bound of the minimum vertex values. Thus, r_{xy} is always positive.

  - **Step 2. Obtain the neighboring minimum and maximum values by checking all cell-averaged values sharing the same vertex point (*i* + 1/2, *j* + 1/2)**

$$u^{\min}_{i+1/2,j+1/2} = \min\left(\bar{u}_{i,j}, \bar{u}_{i+1,j}, \bar{u}_{i,j+1}, \bar{u}_{i+1,j+1}\right),\ u^{\max}_{i+1/2,j+1/2} = \max\left(\bar{u}_{i,j}, \bar{u}_{i+1,j}, \bar{u}_{i,j+1}, \bar{u}_{i+1,j+1}\right)$$

  - **Step 3. Enforce the MLP limiting condition $\phi_{MLP}\left(r\right) = \min\left(\alpha, \alpha r\right)$ onto $u_{i+1/2,j+1/2}$**

$$\bar{u}^{\min}_{i+1/2,j+1/2} \le u_{i+1/2,j+1/2} \le \bar{u}^{\max}_{i+1/2,j+1/2} \text{ or } \bar{u}^{\min}_{i+1/2,j+1/2} \le \bar{u}_{i,j} + \left(1 + r_{xy}\right)\Delta u^{x}_{i+1/2,j} \le \bar{u}^{\max}_{i+1/2,j+1/2}$$

$$\frac{\bar{u}^{\min}_{i+1/2,j+1/2} - \bar{u}_{i,j}}{1 + r_{xy}} \le \Delta u^{x}_{i+1/2,j} \le \frac{\bar{u}^{\max}_{i+1/2,j+1/2} - \bar{u}_{i,j}}{1 + r_{xy}} \text{ or}$$

$$\frac{\bar{u}^{\min}_{i+1/2,j+1/2} - \bar{u}_{i,j}}{1 + r_{xy}} \le 0.5\phi_{MLP}(r_x)\Delta\bar{u}_{i-1/2,j} \le \frac{\bar{u}^{\max}_{i+1/2,j+1/2} - \bar{u}_{i,j}}{1 + r_{xy}} \text{ with } r_x = \Delta\bar{u}_{i+1/2,j} / \Delta\bar{u}_{i-1/2,j}$$

Formulation of MLP on Structured Grids (Cont')

- **Determination of Multi-dimensional Restriction Coefficient, α (cont'd)**
  - **(S4) Obtain the range of α**

If $\Delta u^x_{i+1/2,j} > 0$ (local maximum),

$$0 \le 0.5\phi(r_x)\Delta\bar{u}_{i-1/2,j} \le \frac{\bar{u}^{\max}_{i+1/2,j+1/2} - \bar{u}_{i,j}}{1+r_{xy}} \Rightarrow 0 \le \alpha_{i+1/2,j+1/2} \le \frac{2\max(1,r_x)}{(1+r_{xy})\Delta\bar{u}_{i+1/2,j}}\left(\bar{u}^{\max}_{i+1/2,j+1/2} - \bar{u}_{i,j}\right)$$

If $\Delta u^x_{i+1/2,j} < 0$ (local minimum),

$$\frac{\bar{u}^{\min}_{i+1/2,j+1/2} - \bar{u}_{i,j}}{1+r_{xy}} \le 0.5\phi(r_x)\Delta\bar{u}_{i-1/2,j} \le 0 \Rightarrow 0 \le \alpha_{i+1/2,j+1/2} \le \frac{2\max(1,r_x)}{(1+r_{xy})\Delta\bar{u}_{i+1/2,j}}\left(\bar{u}^{\min}_{i+1/2,j+1/2} - \bar{u}_{i,j}\right)$$

Thus, we have

$$0 \le \alpha_{i+1/2,j+1/2} \le \left|\frac{2\max(1,r_x)}{(1+r_{xy})\Delta\bar{u}_{i+1/2,j}}\right| \min\left(\left|\bar{u}^{\max}_{i+1/2,j+1/2} - \bar{u}_{i,j}\right|, \left|\bar{u}^{\min}_{i+1/2,j+1/2} - \bar{u}_{i,j}\right|\right)$$

By checking four vertex points $(i \pm 1/2, j \pm 1/2)$, we finally have

$$0 \le \alpha \le \left|\frac{2\max(1,r_x)}{(1+r_{xy})\Delta\bar{u}_{i+1/2,j}}\right| \min\left(\left|\bar{u}^{\max}_{i\pm1/2,j\pm1/2} - \bar{u}_{i,j}\right|, \left|\bar{u}^{\min}_{i\pm1/2,j\pm1/2} - \bar{u}_{i,j}\right|\right) \text{ with } r_{xy} = \Delta u^y_{i,j\pm1/2} / \Delta u^x_{i\pm1/2,j}$$

- Note that if $r_{xy} = 0$, α recovers the 1-D TVD form.

Formulation of MLP on Structured Grids (Cont')

- **MLP Slope Limiters**
  - **Cell-interface values in the *x*-direction**

$$u^L_{i+1/2,j} = \bar{u}_{i,j} + 0.5\phi(r_L)\Delta\bar{u}_{i-1/2,j} = \bar{u}_{i,j} + 0.5\max\left(0,\min\left(\alpha_L,\alpha_L r_L,\beta_L\right)\right)\Delta\bar{u}_{i-1/2,j}$$

$$u^R_{i+1/2,j} = \bar{u}_{i+1,j} - 0.5\phi(r_R)\Delta\bar{u}_{i+3/2,j} = \bar{u}_{i+1,j} - 0.5\max\left(0,\min\left(\alpha_R,\alpha_R r_R,\beta_R\right)\right)\Delta\bar{u}_{i+3/2,j}$$

$$\alpha_L = \left|\frac{2\max(1,r_L)}{(1+r_{xy})\Delta\bar{u}_{i+1/2,j}}\right| \min\left(\left|\bar{u}^{\max}_{i\pm1/2,j\pm1/2} - \bar{u}_{i,j}\right|,\left|\bar{u}^{\min}_{i\pm1/2,j\pm1/2} - \bar{u}_{i,j}\right|\right), \quad \alpha_R = \alpha_L\big|_{i\to i+1}$$

with $r_L = \Delta\bar{u}_{i+1/2,j} / \Delta\bar{u}_{i-1/2,j}$ and $r_R = \Delta\bar{u}_{i+1/2,j} / \Delta\bar{u}_{i+3/2,j}$

  - **Choice of local slopes (β)**
    - MLP-van Leer: $\beta_{L\ or\ R} = \dfrac{2r_{L\ or\ R}}{1 + \left|r_{L\ or\ R}\right|}$
    - MLP-superbee: $\beta_{L\ or\ R} = \begin{cases} \min(2r_{L\ or\ R(i-1)},1), & \text{if } 0 < r_{L\ or\ R(i-1)} < 1 \\ \min(r_{L\ or\ R(i-1)},2), & \text{if } r_{L\ or\ R(i-1)} > 1 \end{cases}$ with $r_{R(i-1)} = \dfrac{\Delta\bar{u}_{i-1/2,j}}{\Delta\bar{u}_{i+1/2,j}}$
    - MLP3 (MLP slope limiting with 3rd-order polynomial): $\beta_{L\ or\ R} = \dfrac{1+2r_{L\ or\ R}}{3}$
    - MLP5 (MLP slope limiting with 5th-order polynomial):

$$\beta_L = \frac{-2/r_{L(i-1)} + 11 + 24r_L - 3r_L r_{L(i+1)}}{30}, \quad \beta_R = \frac{-2/r_{R(i+2)} + 11 + 24r_{R(i+1)} - 3r_{R(i+1)} r_R}{30}$$

Maximum Principle and MLP Condition

- **Maximum Principle**
  - **Maximum principle is well-established in parabolic and elliptic PDEs as a tool for L_∞ stability.**
  - **TVD condition, which is a sufficient condition for the maximum principle, is not available in multi-dimensional situation.**
  - **A condition ensuring multi-dimensional monotonicity**
    - Cockburn *et al.* (1990), Liu (1993), Barth (2003), Kim *et al.* (2008, 2010, 2012)
- **L_∞ Stability of MLP Limiting**
  - ***For a multi-dimensional hyperbolic scalar conservation law of***

$$\frac{\partial u}{\partial t}+\frac{\partial f(u)}{\partial x}+\frac{\partial g(u)}{\partial y}=0,$$

the fully discrete scheme using the MLP limiting satisfies the local maximum principle under a suitable CFL condition.

$$\text{If } \overline{u}_{neighbor}^{\min,n} \le \overline{u}_{i,j}^{n} \le \overline{u}_{neighbor}^{\max,n}, \text{ then } \overline{u}_{neighbor}^{\min,n} \le \overline{u}_{i,j}^{n+1} \le \overline{u}_{neighbor}^{\max,n}.$$

Numerical Results

- **A Mach 3 Wind Tunnel with a Step**
  - **A standard test case for high resolution schemes**
  - **Advantage in resolving the slip lines**

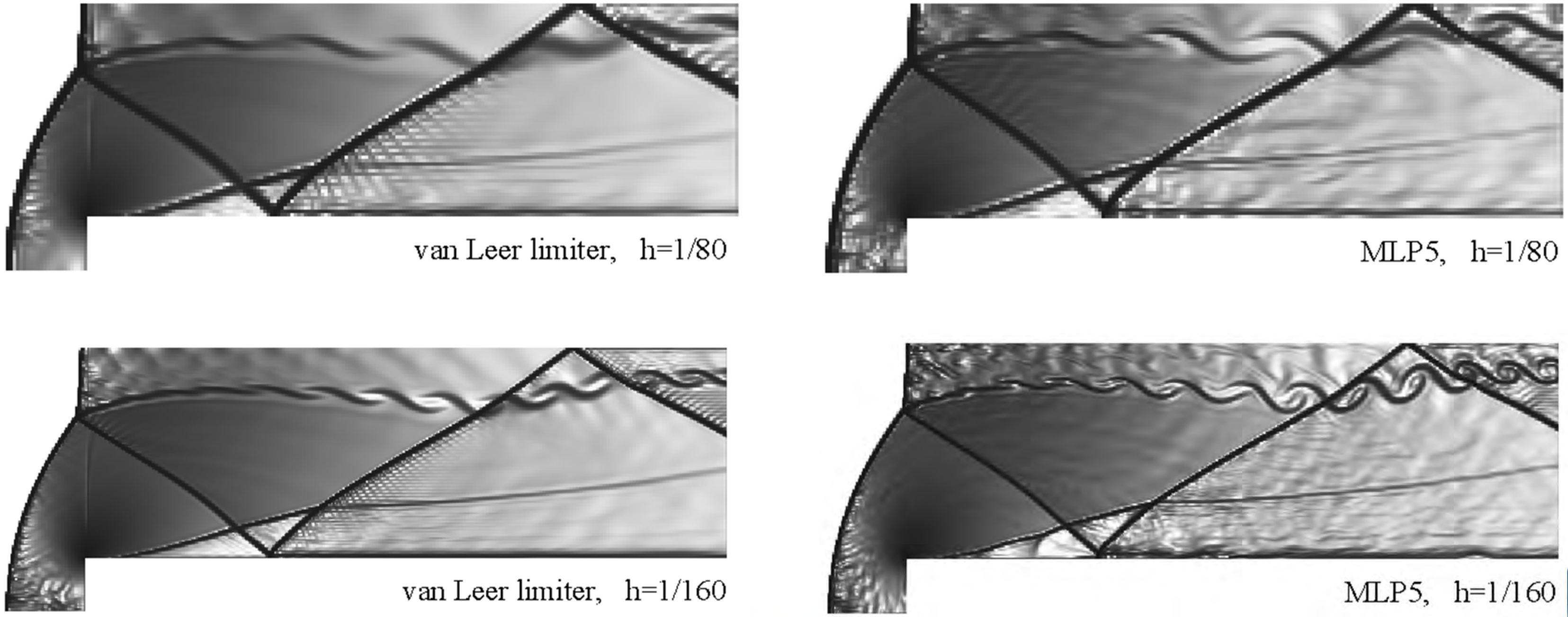

< Numerical Schlieren of a Mach 3 wind tunnel with a step problem >

- **Isentropic Vortex Advection**
  - **Initial mean flow and perturbation values**

$u_\infty = 1,\ \ v_\infty = 1,\ \ p_\infty = \rho_\infty = T_\infty = 1$ with

$$(\delta u, \delta v) = \frac{\beta}{2\pi} e^{(1-r^2)/2}(-\bar{y}, \bar{x}), \delta T = -\frac{(\gamma - 1)\beta^2}{8\gamma\pi^2} e^{1-r^2}.$$

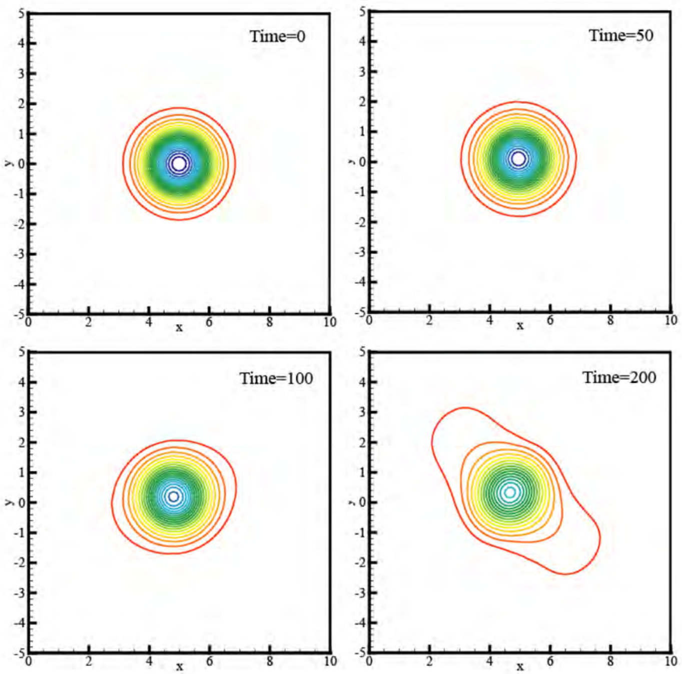

< van Leer limiter >

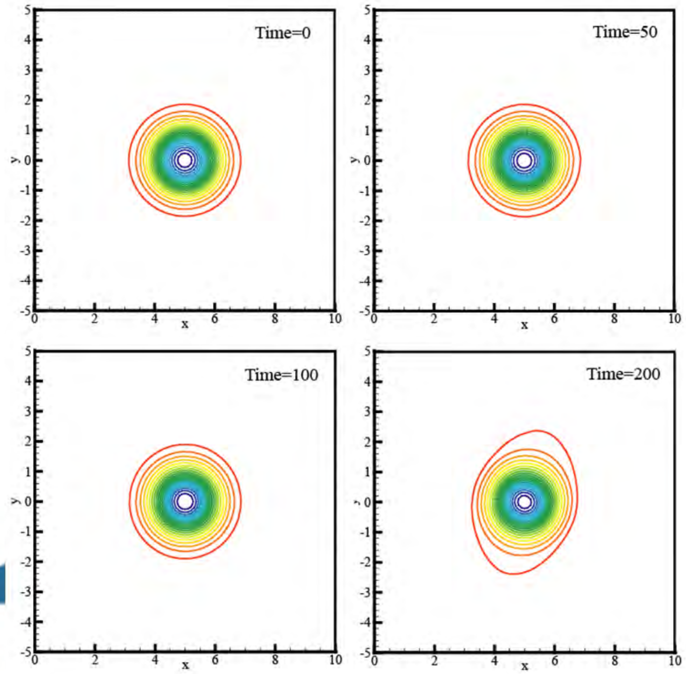

< MLP5 >

Numerical Results (Cont')

Scheme	Size	L_1 error	L_1 order	L_∞ error	L_∞ order
van Leer limiter	50 × 50	4.6165E−03	–	8.9412E−02	–
	100 × 100	1.0489E−03	2.14	2.2579E−02	1.99
	150 × 150	4.5167E−04	2.08	1.0169E−02	1.97
	200 × 200	2.5121E−04	2.04	5.6879E−03	2.02
MLP-van Leer limiter	50 × 50	3.7699E−03	–	8.0859E−02	–
	100 × 100	7.1064E−04	2.41	2.0432E−02	1.98
	150 × 150	2.9575E−04	2.16	9.2804E−03	1.95
	200 × 200	1.5657E−04	2.21	5.1476E−03	2.05
MLP3	50 × 50	2.0713E−03	–	3.9473E−02	–
	100 × 100	2.9620E−04	2.81	7.2746E−03	2.44
	150 × 150	9.8557E−05	2.71	2.9668E−03	2.21
	200 × 200	4.3257E−05	2.86	1.4262E−03	2.55
MLP5	50 × 50	1.1441E−03	–	2.4834E−02	–
	100 × 100	2.2427E−04	2.35	5.5389E−03	2.16
	150 × 150	7.6479E−05	2.65	1.9767E−03	2.54
	200 × 200	4.0756E−05	2.19	1.0291E−03	2.27
Third order polynomial	50 × 50	1.5736E−03	–	4.1150E−02	–
	100 × 100	2.6245E−04	2.58	6.3480E−03	2.70
	150 × 150	9.6728E−05	2.46	2.0090E−03	2.84
	200 × 200	4.9086E−05	2.36	8.9188E−04	2.82

< Grid refinement test >

Numerical Results (Cont')

- **Three-dimensional Normal Shock Discontinuity**
  - **Examine the shock-capturing characteristics of TVD and MLP**
  - **Normal shock discontinuity inclined by 45 degree angle to each cell-surface**

< Density contour >

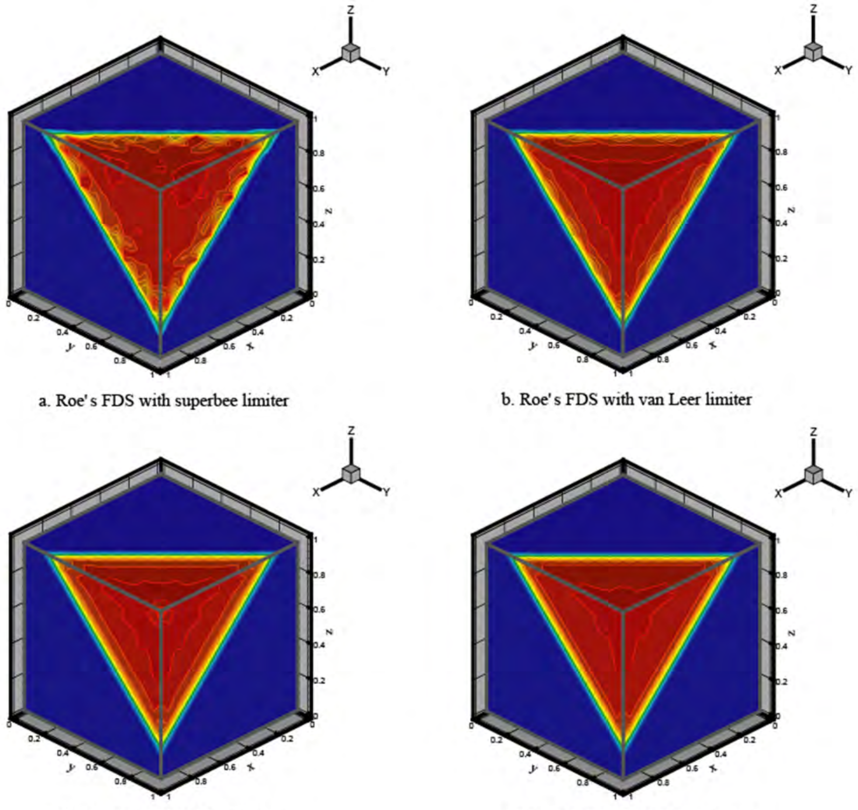

a. Roe's FDS with superbee limiter

b. Roe's FDS with van Leer limiter

c. Roe's FDS with MLP-superbee

d. Roe's FDS with MLP-van Leer

< Error history >

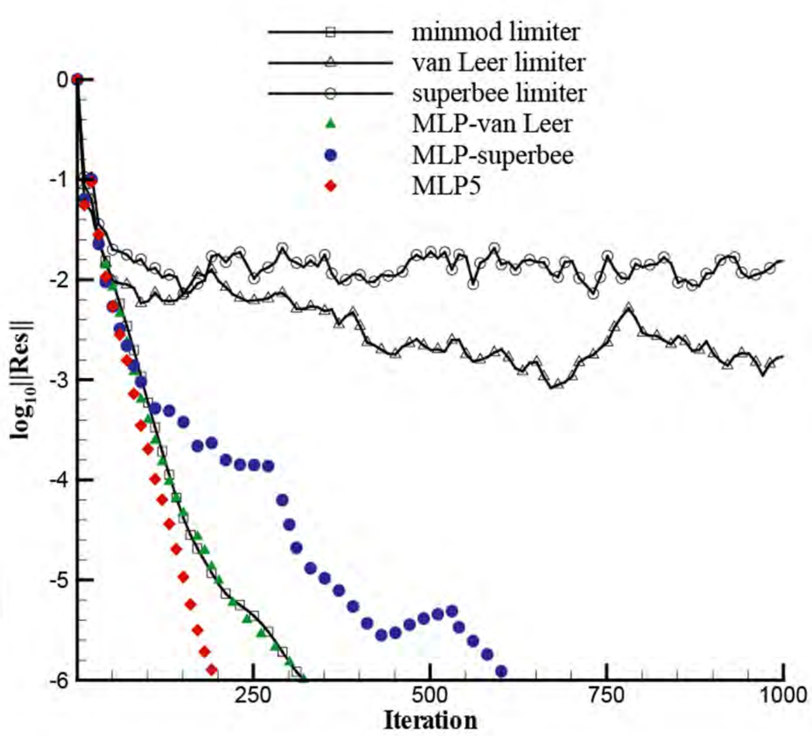

Numerical Results (Cont')

- **Three-dimensional Pure Vortex Flow**
  - **A simple model of a tip vortex element released from a rotor blade.**
    - Thomson-Rankine vortex model with 50 x 50 x 50 grids

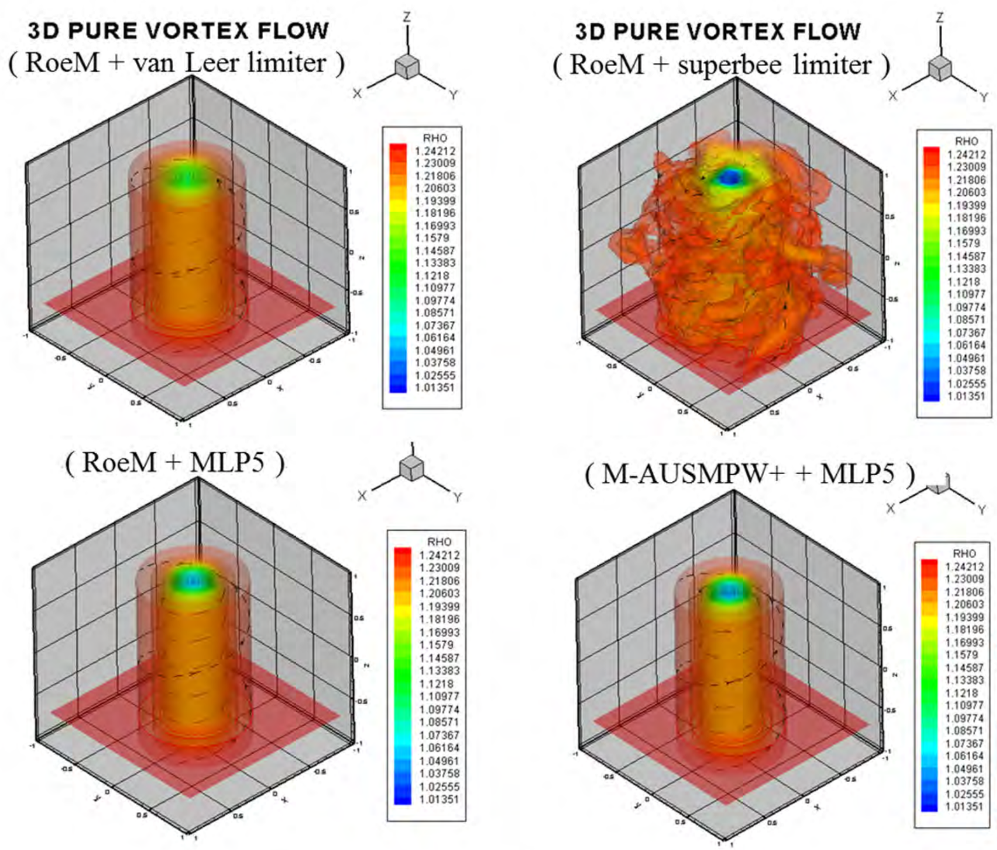

< Density contours at non-dimensional time 20.0 >

$$v_\theta = \begin{cases} \omega r \;, & r < a \\ \dfrac{\omega a^2}{r} \;, & r > a \end{cases} \quad \text{with } \omega = \text{const}$$

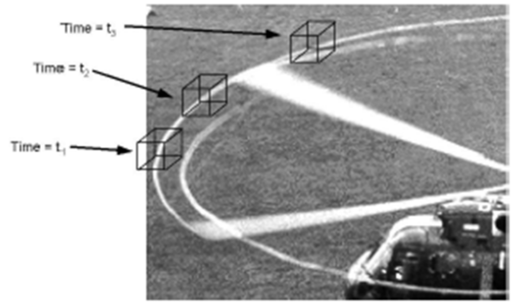

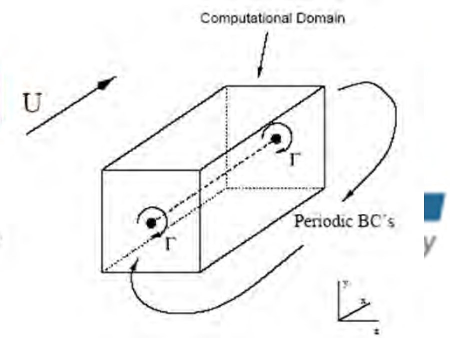

Numerical Results (Cont')

- **The Case of Vortex Core Aligned with z-axis**

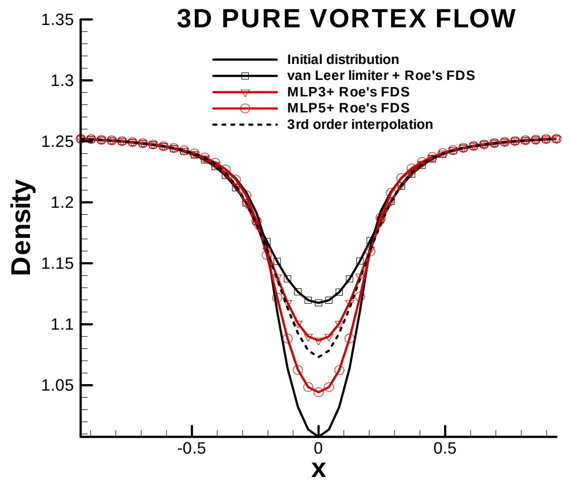

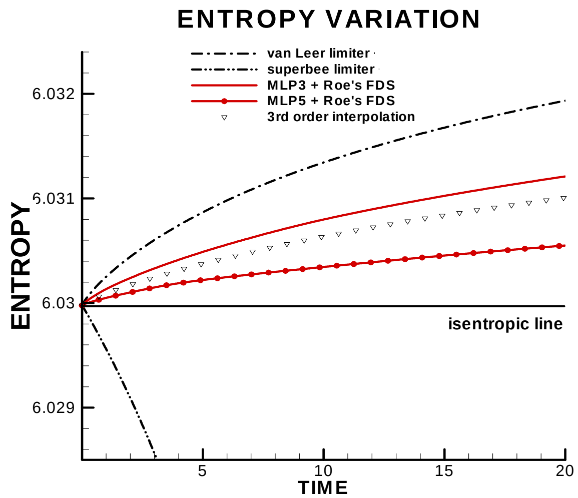

- **The Case of Vortex Core Non-aligned with z-axis**

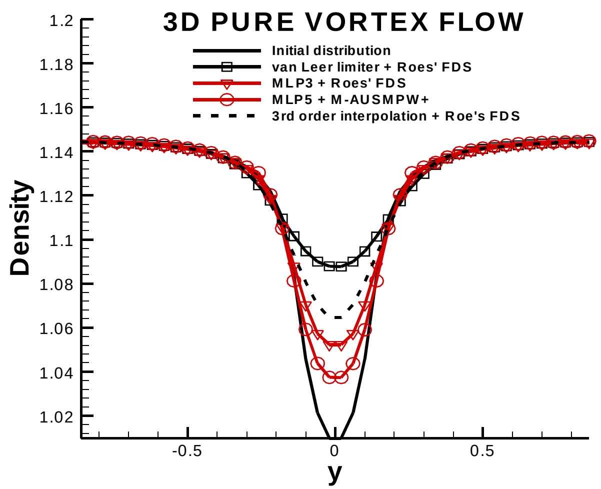

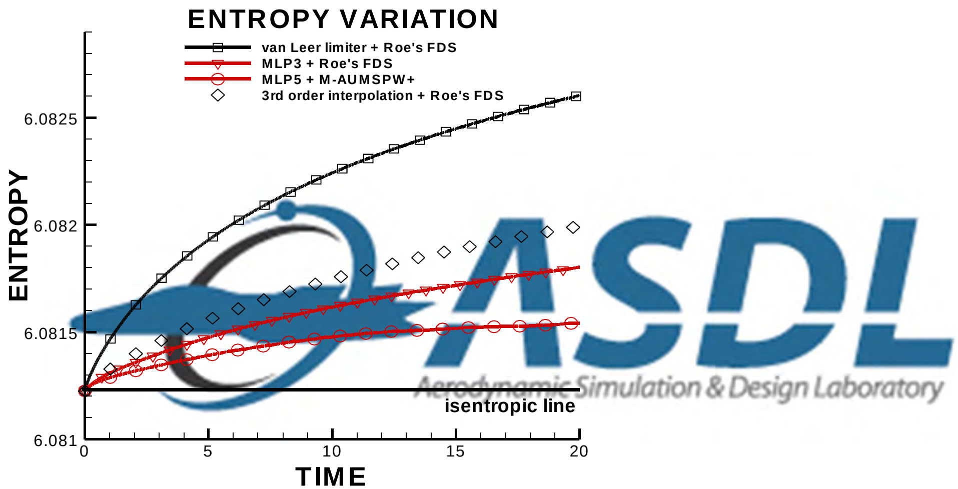

Numerical Results (Cont')

- **Laminar Shock-Boundary Layer Interaction**
  - **Free stream Mach number : $M_\infty = 2.0$, shock impinging angle : $\theta = 32.585$ degree**
  - **Reynolds number : Re = 2.96×10^5**
  - **Grid system : 56 × 59, 150 × 200**

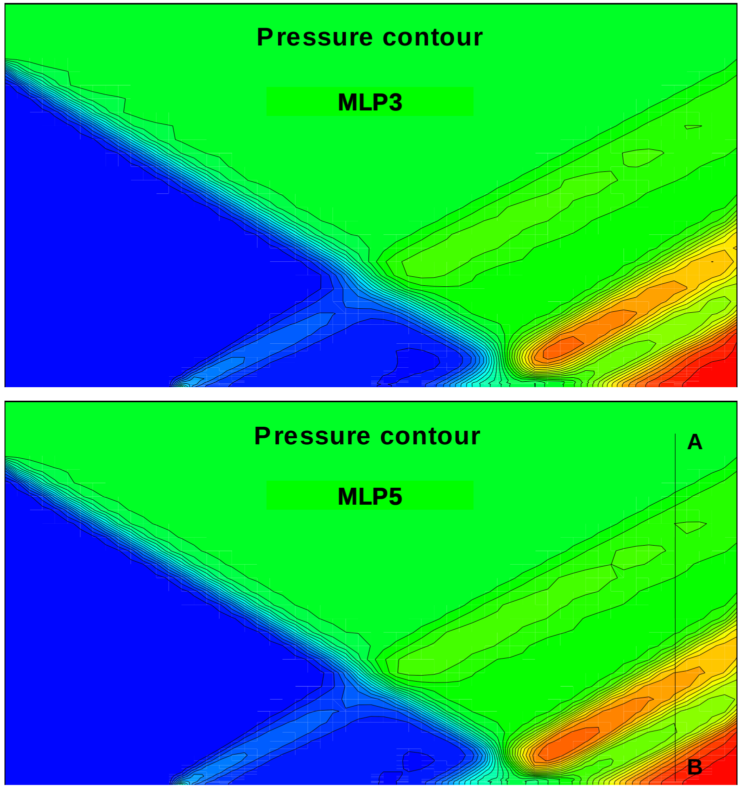

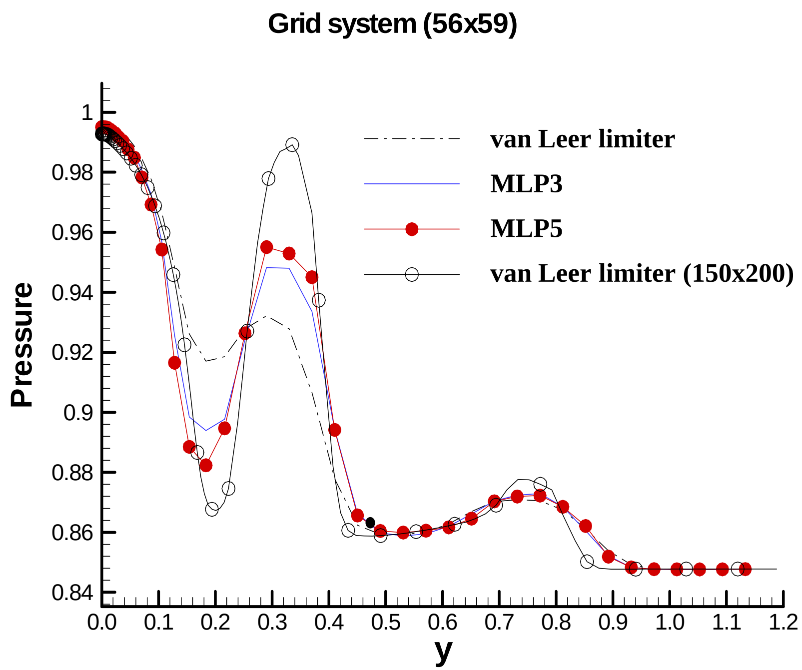

< Comparison of pressure distribution along line AB >

Numerical Results (Cont')

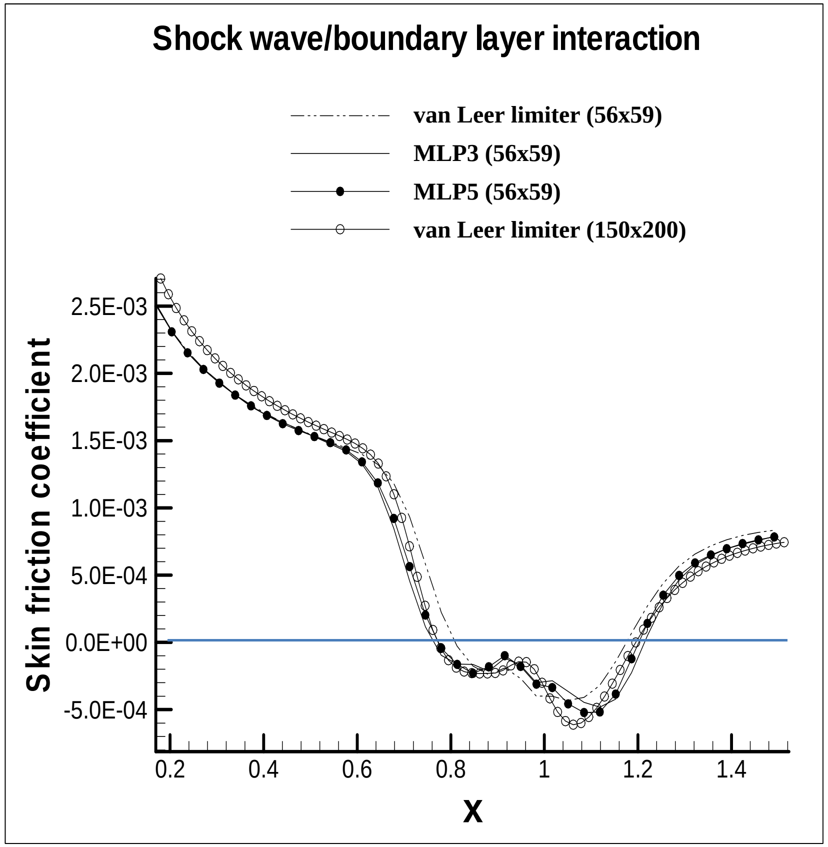

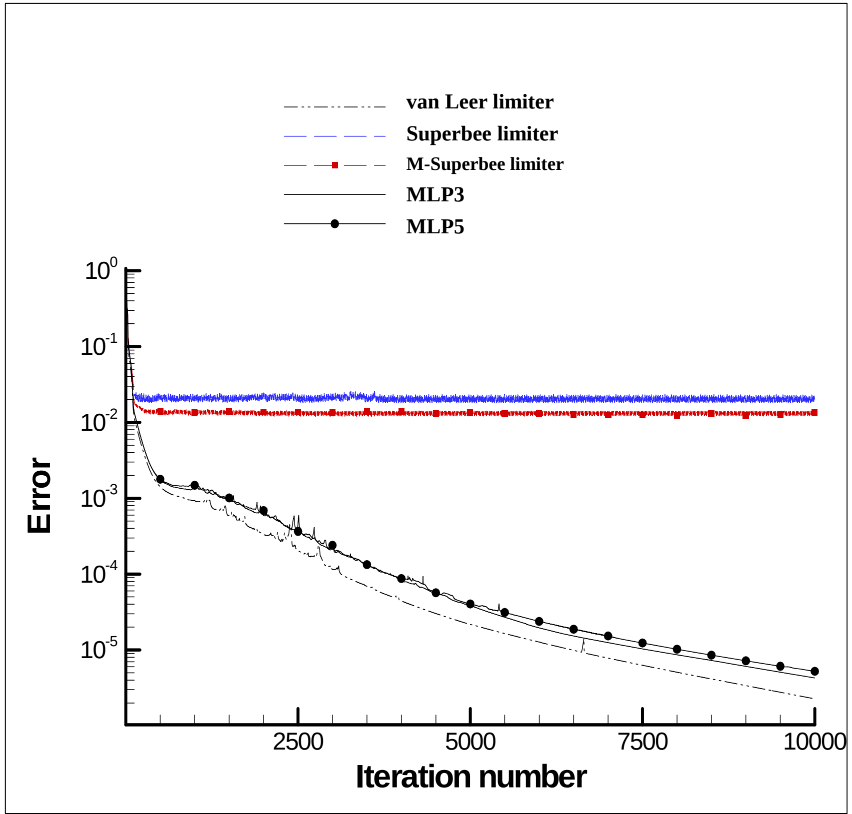

< Skin friction coefficient and error history >

- **3-D Viscous Shock Tube Problem**
  - **Computed conditions**
    - Spatial discretization
      - AUSMPW+, M-AUSMPW+
    - Time integration
      - 3rd-order TVD Runge-Kutta
    - Grid system
      - 250x125x125, 350x175x175, 500x250x250
    - Reynolds number: 200 with constant viscosity
    - Boundary values
      - No slip B.C (x=0, x=1, y=0, z=0)
      - Symmetric B.C (y=0.5, z=0.5)

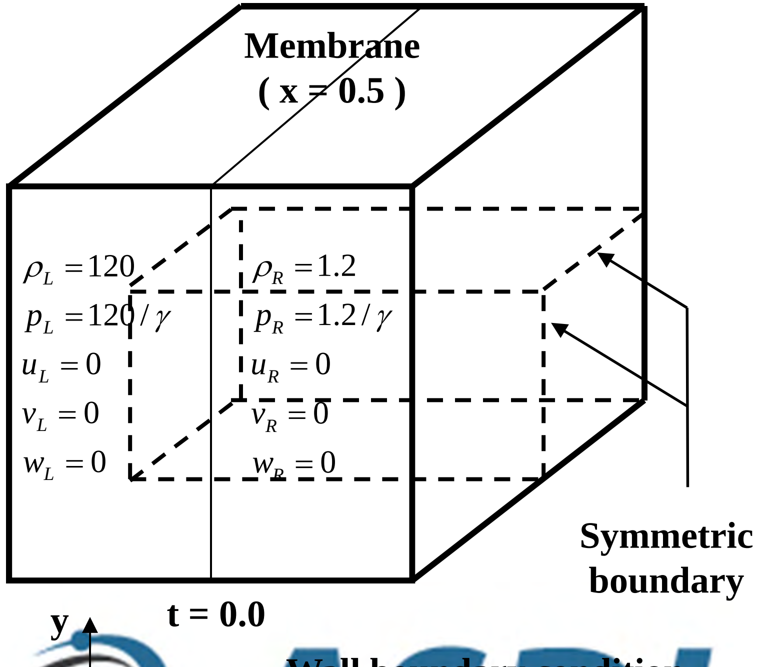

Numerical Results (Cont')

- **Profiles of 3-D Viscous Shock Tube Problem**
  - Complicated shock-boundary interaction, and vortical structure

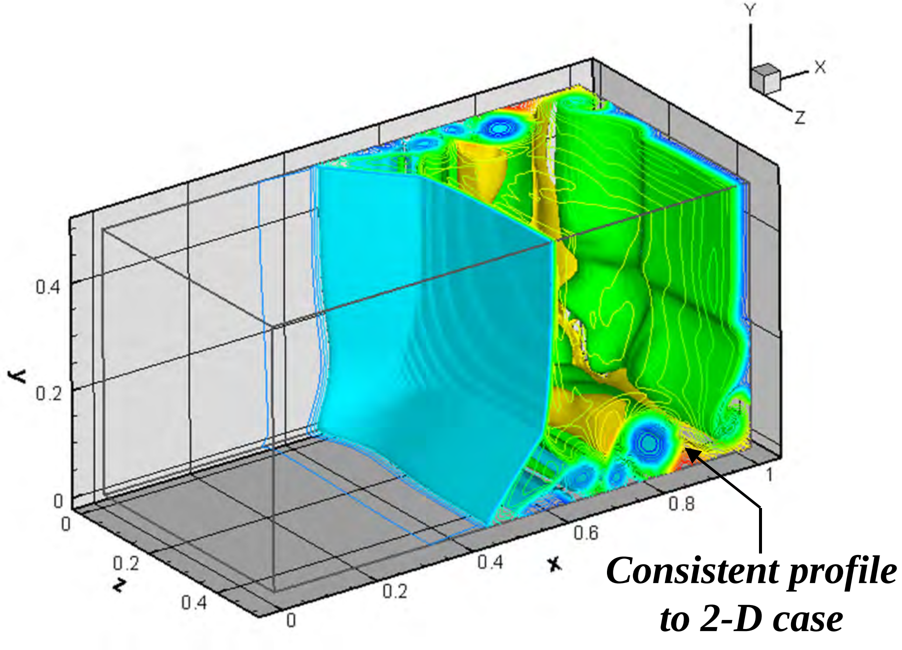

Consistent profile to 2-D case

< Density contour : t = 1.0 >

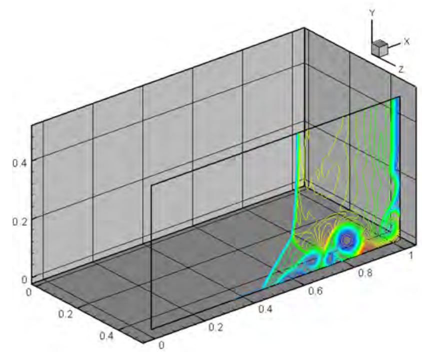

< xy-plane contour >

Near the wall, distinct 3-D vortex structure

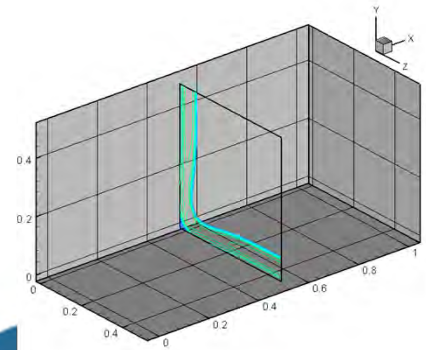

< yz-plane contour >

Similar to corner flow, built-up swirl flow

Comparison : profile of separated vortex

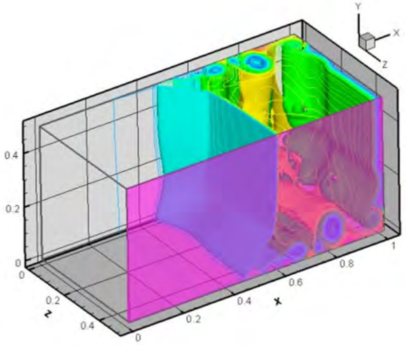

	No. of grid pts.
Coarse mesh	3,906,250 (250x125x125)
Medium mesh	10,718,750 (350x175x175)
Fine mesh	31,250,000 (500x250x250)

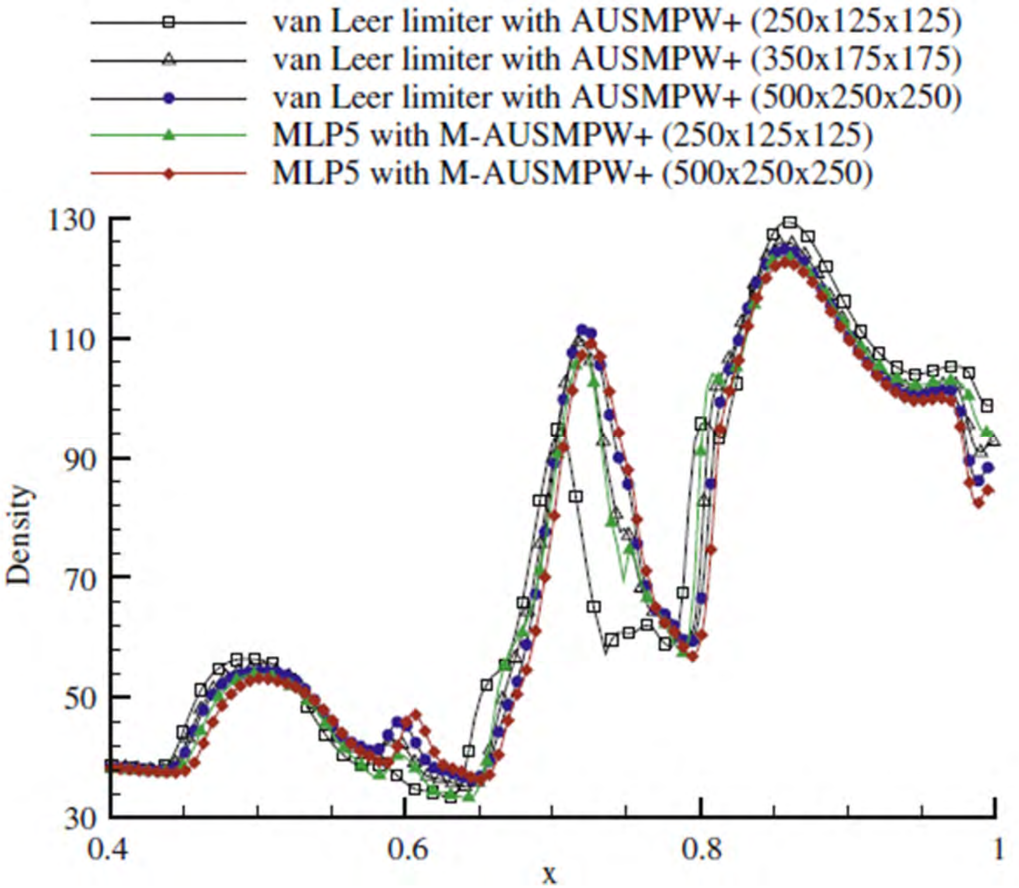

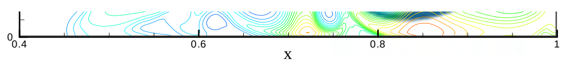

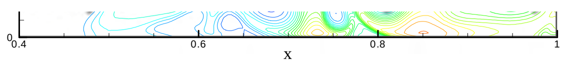

Concluding Remarks

- **In order to obtain high-resolution flow structure, higher-order numerical scheme is essential.**
  - **Treatment of discontinuous and smooth region in multiple dimensions**

- **From one- to multi-dimensional flows, a limiting process must include to the treatment of vertex to efficiently include a missing flow physics at 1-D based limiting strategy.**
  - **Overcome the weakness of dimensional splitting approach, and eliminate spurious oscillations caused by multi-dimensional discontinuity.**

- **Characteristics of MLP**
  - **Multi-dimensional monotonicity guided by the MLP condition and the discrete maximum principle → L_∞ stability**
  - **Slopes based on higher-order polynomial reconstruction**
  - **Computational efficiency comparable to conventional TVD limiters**
  - **Enhanced accuracy and convergence characteristics**